Document made available under the Patent Cooperation Treaty (PCT)

International application number: PCT/US05/002848

International filing date: 02 February 2005 (02.02.2005)

Document type: Certified copy of priority document

Document details: Country/Office: US
Number: 60/541,531
Filing date: 03 February 2004 (03.02.2004)

Date of receipt at the International Bureau: 09 May 2005 (09.05.2005)

Remark: Priority document submitted or transmitted to the International Bureau in compliance with Rule 17.1(a) or (b)

1314574

THE UNITED STATES OF AMERICA

TO ALL TO WHOM THESE PRESENTS SHALL COME:

UNITED STATES DEPARTMENT OF COMMERCE

United States Patent and Trademark Office

April 27, 2005

THIS IS TO CERTIFY THAT ANNEXED HERETO IS A TRUE COPY FROM THE RECORDS OF THE UNITED STATES PATENT AND TRADEMARK OFFICE OF THOSE PAPERS OF THE BELOW IDENTIFIED PATENT APPLICATION THAT MET THE REQUIREMENTS TO BE GRANTED A FILING DATE.

APPLICATION NUMBER: *60/541,531*
FILING DATE: *February 03, 2004*
RELATED PCT APPLICATION NUMBER: *PCT/US05/02848*

Certified by

Jon W. Dudas

Under Secretary of Commerce
for Intellectual Property
and Director of the United States
Patent and Trademark Office

PROVISIONAL APPLICATION FOR PATENT COVER SHEET

This is a request for filing a PROVISIONAL APPLICATION FOR PATENT under 37 CFR 1.53(c).

Express Mail Label No. EL984956883US

INVENTOR(S)		
Given Name (first and middle [if any])	Family Name or Surname	Residence (City and either State or Foreign Country)
Robert	Gilmour, Jr.	208 Hanshaw Road Ithaca, New York 14850
Jeffrey J.	Fox	118 Blair Street, Apt. 1 Ithaca, New York 14850
Mark	Riccio	100 Graham Road, 12A Ithaca, New York 14850

☐ *Additional inventors are being named on the ____ separately numbered sheets attached hereto*

TITLE OF THE INVENTION (280 characters max)

STIMULATION PROTOCOL FOR INITIATION OF VENTRICULAR FIBRILLATION: 3 METHODS FOR DECREASING THE RISK OF VF INITIATION

Direct all correspondence to: **CORRESPONDENCE ADDRESS**

☐ Customer Number [ ] → *Place Customer Number Bar Code Label here*

OR *Type Customer Number here*

☒ Firm *or* Individual Name	Michael L. Goldman Nixon Peabody LLP				
Address	Clinton Square, P.O. Box 31051				
City	Rochester	State	NY	ZIP	14603-1051
Country	USA	Telephone	(585) 263-1304	Fax	(585) 263-1600

ENCLOSED APPLICATION PARTS ***(check all that apply)***

☒ Specification *Number of Pages* 43 ☐ CD(s), Number [ ]

☐ Drawing(s) *Number of Sheets* [ ] ☐ Other (specify) [ ]

☐ Application Data Sheet. See 37 CFR 1.76

METHOD OF PAYMENT OF FILING FEES FOR THIS PROVISIONAL APPLICATION FOR PATENT

☒ Applicant claims small entity status. See 37 CFR 1.27.

☐ A check or money order is enclosed to cover the filing fees

☒ The Commissioner is hereby authorized to charge fees which may be required, or credit any overpayment to Deposit Account Number: 14-1138

☐ Payment by credit card. Form PTO-2038 is attached.

FILING FEE AMOUNT ($): $80.00

The invention was made by an agency of the United States Government or under a contract with an agency of the United States Government.

☐ No.

☒ Yes, the name of the U.S. Government agency and the Government contract number are: **NIH, Contract No. HL62543**

Respectfully submitted, Date 2/3/04

SIGNATURE Michael L. Goldman

REGISTRATION NO. *(if appropriate)* 30,727

TYPED or PRINTED NAME Michael L. Goldman

Docket Number: 19603/4610 (CRF D-3318-01)

TELEPHONE (585) 263-1304

USE ONLY FOR FILING A PROVISIONAL APPLICATION FOR PATENT

Mail Stop Provisional Patent Application
Commissioner for Patents
P.O. Box 1450
Alexandria, VA 22313-1450

R746379.1

FEE TRANSMITTAL FOR FY 2004

Patent fees are subject to annual revision.

☒ Applicant claims small entity status. See 37 CFR 1.27

TOTAL AMOUNT OF PAYMENT ($) 80

Complete if Known	
Application Number	To be Assigned
Filing Date	Herewith
First Named Inventor	Gilmour et al.
Examiner Name	
Art Unit	
Attorney Docket No.	19603/4610 (CRF D-3318-01)

METHOD OF PAYMENT *(check all that apply)*

☐ Check ☐ Credit Card ☐ Money Order ☐ Other ☐ None

☒ Deposit Account:

Deposit Account Number: 14-1138

Deposit Account Name: Nixon Peabody LLP

The Commissioner is authorized to: *(check all that apply)*

☒ Charge fee(s) indicated below ☒ Credit any overpayments

☒ Charge any additional fee(s)

☐ Charge fee(s) indicated below, **except for the filing fee** to the above-identified deposit account.

FEE CALCULATION

1. BASIC FILING FEE

Large Entity Fee Code	Large Entity Fee ($)	Small Entity Fee Code	Small Entity Fee ($)	Fee Description	Fee Paid
1001	770	2001	385	Utility filing fee	
1002	340	2002	170	Design filing fee	
1003	530	2003	265	Plant filing fee	
1004	770	2004	385	Reissue filing fee	
1005	160	2005	80	Provisional filing fee	80

SUBTOTAL (1) ($) 80

2. EXTRA CLAIM FEES FOR UTILITY AND REISSUE

			Extra Claims		Fee from below		Fee Paid
Total Claims		-20** =		X		=	0
Independent Claims		-3** =		X		=	0
Multiple Dependent				X		=	0

Large Entity Fee Code	Large Entity Fee ($)	Small Entity Fee Code	Small Entity Fee ($)	Fee Description
1202	18	2202	9	Claims in excess of 20
1201	86	2201	43	Independent claims in excess of 3
1203	290	2203	145	Multiple dependent claim, if not paid
1204	86	2204	43	** Reissue independent claims over original patent
1205	18	2205	9	** Reissue claims in excess of 20 and over original patent

SUBTOTAL (2) ($) 0

**or number previously paid, if greater; For Reissues, see above

FEE CALCULATION (continued)

3. ADDITIONAL FEES

Large Entity Fee Code	Large Entity Fee ($)	Small Entity Fee Code	Small Entity Fee ($)	Fee Description	
1051	130	2051	65	Surcharge – late filing fee or oath	
1052	50	2052	25	Surcharge - late provisional filing fee or cover sheet	
1053	130	1053	130	Non-English specification	
1812	2,520	1812	2,520	For filing a request for *ex parte* reexamination	
1804	920*	1804	920*	Requesting publication of SIR prior to Examiner action	
1805	1,840*	1805	1,840*	Requesting publication of SIR after Examiner action	
1251	110	2251	55	Extension for reply within first month	
1252	420	2252	210	Extension for reply within second month	
1253	950	2253	475	Extension for reply within third month	
1254	1,480	2254	740	Extension for reply within fourth month	
1255	2,010	2255	1,005	Extension for reply within fifth month	
1401	330	2401	165	Notice of Appeal	
1402	330	2402	165	Filing a brief in support of an appeal	
1403	290	2403	145	Request for oral hearing	
1451	1,510	1451	1,510	Petition to institute a public use proceeding	
1452	110	2452	55	Petition to revive – unavoidable	
1453	1,330	2453	665	Petition to revive – unintentional	
1501	1,330	2501	665	Utility issue fee (or reissue)	
1502	480	2502	240	Design issue fee	
1503	640	2503	320	Plant issue fee	
1460	130	1460	130	Petitions to the Commissioner	
1807	50	1807	50	Processing fee under 37 CFR 1.17(q)	
1806	180	1806	180	Submission of Information Disclosure Stmt	
8021	40	8021	40	Recording each patent assignment per property (times number of properties)	
1809	770	2809	385	Filing a submission after final rejection (37 CFR 1.129(a))	
1810	770	2810	385	For each additional invention to be examined (37 CFR 1.129(b))	
1801	770	2801	385	Request for Continued Examination (RCE)	
1802	900	1802	900	Request for expedited examination of a design application	

Other fee (specify) _____

*Reduced by Basic Filing Fee Paid

SUBTOTAL (3) ($) 0

CERTIFICATE OF MAILING OR TRANSMISSION [37 CFR 1.8(a)]

I hereby certify that this correspondence is being:

☐ deposited with the United States Postal Service on the date shown below with sufficient postage as first class mail in an envelope addressed to: Mail Stop _____, Commissioner for Patents, P. O. Box 1450, Alexandria, VA 22313-1450

☐ transmitted by facsimile on the date shown below to the United States Patent and Trademark Office at (703) _____.

Date _____ Signature _____

Typed or printed name _____

SUBMITTED BY

				Complete *(if applicable)*	
Name *(Print/Type)*	Michael L. Goldman	Registration No. *(Attorney/Agent)*	30,727	Telephone	(585) 263-1304
Signature	Michael L. Goldman			Date	February 3, 2004

SEND TO: Commissioner for Patents
P.O. Box 1450
Alexandria, VA 22313-1450

R746381.1

EXPRESS MAIL CERTIFICATE

DOCKET NO.: **19603/4610 (CRF D-3318-01)**

APPLICANTS: **Robert Gilmour, Jr., Jeffrey J. Fox, Mark Riccio**

TITLE: **STIMULATION PROTOCOL FOR INITIATION OF VENTRICULAR FIBRILLATION: 3 METHODS FOR DECREASING THE RISK OF VF INITIATION**

Certificate is attached to the **Provisional Application for Patent Cover Sheet (1 page) and Fee Transmittal (1 page)** of the above-identified application.

"EXPRESS MAIL" NUMBER: **EL984956883US**
DATE OF DEPOSIT: **February 3, 2004**

I hereby certify that this paper or fee is being deposited with the United States Postal Service "Express Mail Post Office to Addressee" service under 37 CFR 1.10 on the date indicated above and is addressed to Mail Stop Provisional Patent Application, Commissioner for Patents, P.O. Box 1450, Alexandria, VA 22313-1450.

Shawn A. Lockett
(Typed or Printed Name of Person Mailing Paper or Fee)

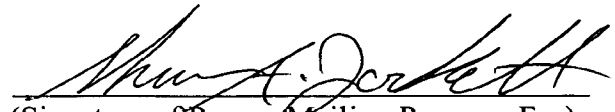

(Signature of Person Mailing Paper or Fee)

EXPRESS MAIL CERTIFICATE

DOCKET NO.: **19603/4610 (CRF D-3318-01)**

APPLICANTS: **Robert Gilmour, Jr., Jeffrey J. Fox, Mark Riccio**

TITLE: **STIMULATION PROTOCOL FOR INITIATION OF VENTRICULAR FIBRILLATION: 3 METHODS FOR DECREASING THE RISK OF VF INITIATION**

Certificate is attached to the **Provisional Patent Application (43 pages)** of the above-identified application.

"EXPRESS MAIL" NUMBER: **EL984956883US**
DATE OF DEPOSIT: **February 3, 2004**

I hereby certify that this paper or fee is being deposited with the United States Postal Service "Express Mail Post Office to Addressee" service under 37 CFR 1.10 on the date indicated above and is addressed to Mail Stop Provisional Patent Application, Commissioner for Patents, P.O. Box 1450, Alexandria, VA 22313-1450.

Shawn A. Lockett
(Typed or Printed Name of Person Mailing Paper or Fee)

(Signature of Person Mailing Paper or Fee)

BEST AVAILABLE IMAGES

Defective images within this document are accurate representations of the original documents submitted by the applicant.

Defects in the images may include (but are not limited to):

- BLACK BORDERS
- TEXT CUT OFF AT TOP, BOTTOM OR SIDES
- FADED TEXT
- ILLEGIBLE TEXT
- SKEWED/SLANTED IMAGES
- COLORED PHOTOS
- BLACK OR VERY BLACK AND WHITE DARK PHOTOS
- GRAY SCALE DOCUMENTS

IMAGES ARE BEST AVAILABLE COPY.

As rescanning documents *will not* correct images, please do not report the images to the Image Problem Mailbox.

TITLE: **STIMULATION PROTOCOL FOR INITIATION OF VENTRICULAR FIBRILLATION: 3 METHODS FOR DECREASING THE RISK OF VF INITIATION**

INVENTORS: **Robert Gilmour, Jr., Jeffrey J. Fox, Mark Riccio**

DOCKET NO.: **19603/4610 (CRF D-3318-01)**

PROVISIONAL PATENT APPLICATION

A novel approach to identifying antiarrhythmic drug targets

Sudden cardiac death, secondary to ventricular fibrillation (VF), remains the leading cause of death in the USA. Recent experimental and theoretical studies suggest that VF could be caused by spiral wave re-entry. The initiation and subsequent break-up of spiral waves has been linked to electrical alternans, a phenomenon produced in cardiac tissue that has a steeply sloped restitution relation. Agents that reduce the slope of the restitution relation have been shown to suppress alternans and, presumably by that mechanism, terminate VF. These results suggest that electrical restitution could be a promising new target for antiarrhythmic therapies.

▼ Catastrophic rhythm disturbances of the heart, such as ventricular fibrillation (VF), are the major cause of death in the United States [1,2]. Treatment of these rhythm disorders remains largely empirical, in part because of an incomplete understanding of underlying cellular electrophysiological mechanisms. Recent studies, building on earlier theoretical work by Krinsky, Winfree and colleagues [3,4] and experiments by Allessie [5], have suggested that spiral wave re-entry could be the 'engine' that drives VF [6–11]. Although there is substantial evidence that spiral wave re-entry contributes significantly to the induction and maintenance of VF, the exact mechanism by which spiral waves sustain VF is currently being debated. Correctly identifying the mechanism (or, more likely, mechanisms) by which spiral waves cause VF is likely to be a crucial step in the development of pharmacological approaches to VF prevention.

Restitution hypothesis for VF

One of the hypotheses to account for the apparent link between spiral waves and VF is the restitution hypothesis, which proposes that VF is caused by the break up of a single spiral wave into multiple self-perpetuating wavelets [8,10,12–17]. This mechanism is similar to that proposed decades ago by Moe [18], but with one important difference: it can occur in intrinsically homogeneous cardiac tissue (for reasons to be described below). The transition from normal planar wave excitation to a single spiral wave and, ultimately, to multiple wavelets is thought to underlie the transition from normal sinus rhythm to ventricular tachycardia and VF characteristic of patients who succumb to sudden death (Fig. 1).

The exact mechanism for the break up of spiral waves is unknown. However, there is considerable evidence that break up is closely related to action potential duration (APD) restitution, which is the relationship between APD and diastolic interval (DI, the time interval between action potentials), in which APD is determined by the preceding DI (Fig. 2). During pacing of cardiac tissue at progressively shorter cycle lengths, APD decreases, until at sufficiently short cycle lengths a period-doubling bifurcation occurs and APD begins to alternate between a long duration and a short duration, a phenomenon known as APD alternans (Fig. 2) [19–24]. The development of APD alternans requires that the slope of the restitution relation exceeds 1, whereas if the slope of the restitution is less than 1, alternans will not occur.

The slope of the restitution relation, and the corresponding presence or absence of APD alternans, has been linked to spiral wave stability. If the slope of the APD restitution relation is <1, a spiral wave tends to stabilize and produce a periodic rhythm, the manifestation of which might be monomorphic ventricular tachycardia. If, however, the slope of the APD restitution relation is ≥ 1, a single spiral wave might disintegrate into many spiral waves, manifested as VF. These transitions are illustrated in Fig. 3, using results generated by a computer model. Once initiated, a single stable spiral wave can be destabilized by increasing the slope of the restitution relation from <1 to ≥ 1. Similarly, multiple wavelets can be induced to coalesce into a single spiral wave

by reducing the slope of the restitution relation from ≥1 to <1. Thus, a reduction f the slope of the restitution relation from ≥1 to <1 is expected to prevent the induction of VF and to convert existing VF into a periodic rhythm.

Several recent studies have provided experimental and theoretical support for a causal relationship between APD restitution and VF [12,13,25–29]. If the APD restitution relation contains a region of slope ≥1, APD alternans and VF are induced by pacing at short cycle lengths. If the slope of the APD restitution relation is reduced to less than one, APD alternans is suppressed and VF is not induced. Furthermore, if a fibrillating ventricle is exposed to a drug that reduces the slope of the restitution to less than 1, VF is converted to a periodic rhythm sustained by a single stable spiral wave [12,13,26].

Unfortunately, interventions that suppress VF experimentally (verapamil [13], bretylium [12] and hyperkalemia [26]) have unwanted actions that severely limit their clinical use. Nevertheless, the effects of these interventions on restitution and VF have provided valuable insights regarding new, potentially more clinically relevant, drug targets. In particular, attempts to understand the mechanism by which calcium channel blockers alter APD restitution have led to the realization that increasing selected outward repolarizing currents might also flatten restitution, as discussed in the following sections.

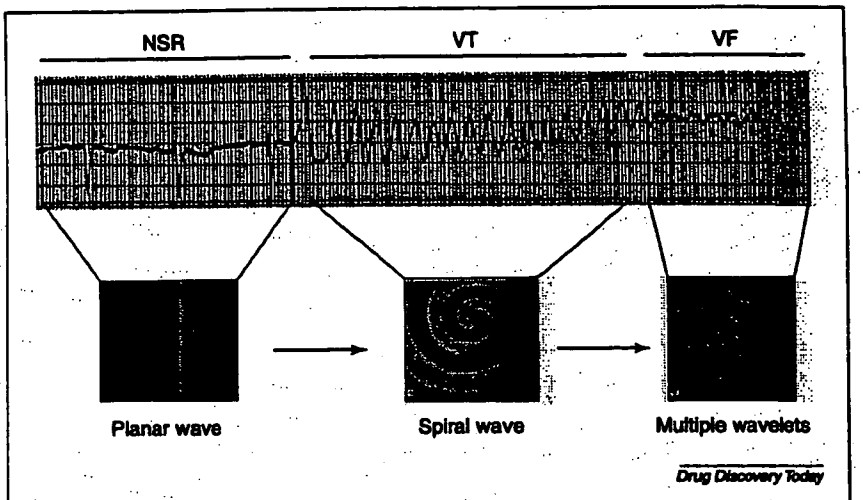

Figure 1. Proposed evolution of cardiac wave propagation patterns underlying the transition from a normal cardiac rhythm to ventricular fibrillation. Transition from normal sinus rhythm (NSR) to ventricular tachycardia (VT) and ventricular fibrillation (VF), as recorded on the surface electrocardiogram. Corresponding transitions from a planar wave to a single spiral wave to multiple spiral waves.

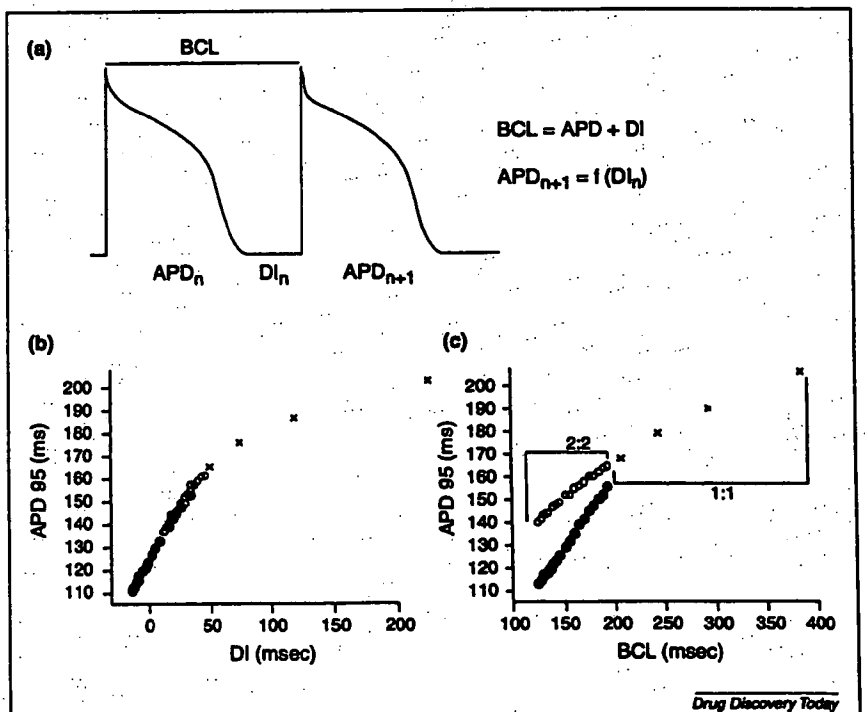

Figure 2. Restitution of action potential duration (APD). (a) Definition of APD, diastolic interval (DI) and cycle length (CL). The duration of the n+1th action potential (APD$_{n+1}$) is a function of the preceding DI (DI$_n$). (b) Plot of APD versus preceding DI. (c) Plot of APD versus CL. Crosses are APDs during the CLs in which no alternans occurs. During APD alternans, unfilled circles are APDs during the long action potential, and filled circles are APDs during the short action potential. Modified, with permission, from Koller *et al.* [25].

Calcium channel antagonists and VF

The suppression of VF by verapamil, in association with a reduction in the slope of the APD restitution relation (Fig. 4), suggests that the L-type calcium current (I_{Ca}) has a key role in restitution and in the development of VF [13,30]. To better define these roles, we recently developed an ionic model for the cardiac ventricular myocyte (CVM) based on the Winslow [31] and Luo–Rudy models [32] that generates physiologically realistic

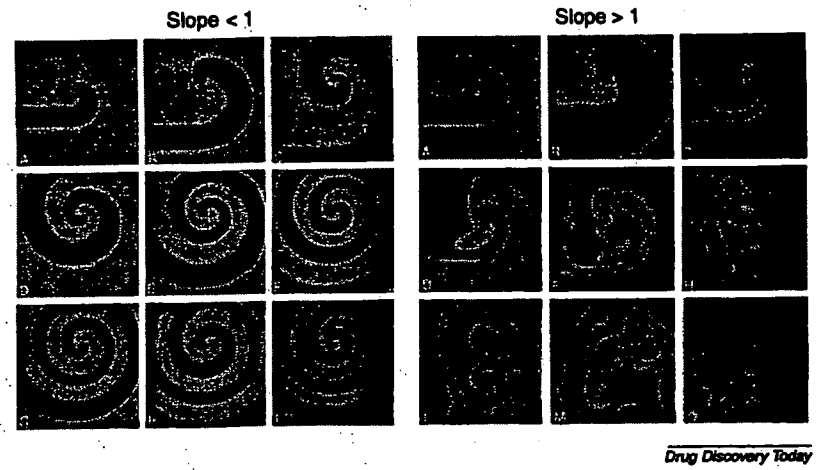

Figure 3. Wave patterns in a computer model of cardiac activation. Sequential snapshots (A–I) of activation during the development of a stable single spiral wave under conditions in which the slope of the restitution relation for action potential duration is <1 (left panel). The transition from a single spiral wave into many spiral waves for a restitution slope >1 (A–O, with some intervening steps deleted: right panel). Results courtesy of Dante R. Chialvo (Department of Physiology, University of California, Los Angeles: http://www.ucla.edu).

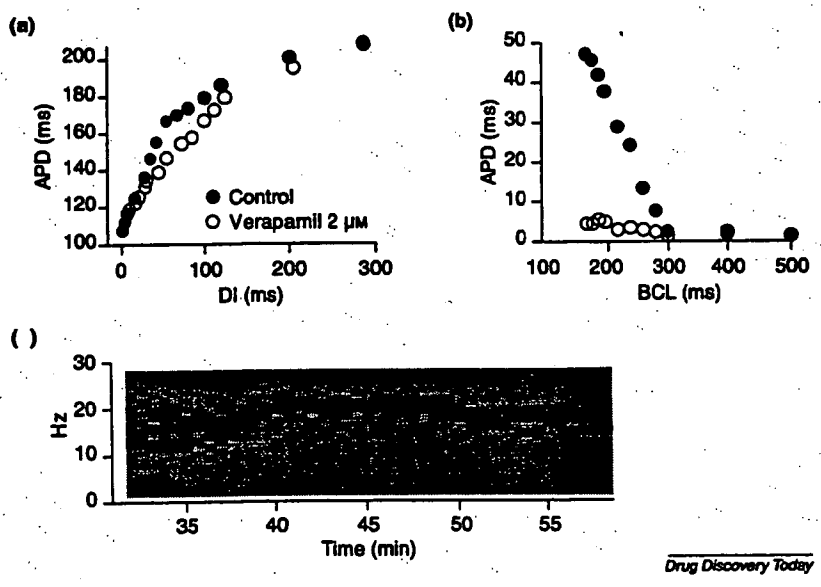

Figure 4. Effects of verapamil on action potential duration (APD) restitution and ventricular fibrillation (VF). (a) Example of the reduction in the slope of the APD restitution relation after exposure to verapamil. (b) Corresponding reduction in the magnitude of APD alternans (AM) during pacing at different basic cycle lengths (BCL) after exposure to verapamil. (c) Effects of verapamil on the composite Fast Fourier Transform (FFT) of monophasic action potential (MAP) recordings during VF in arterially perfused canine ventricle. Verapamil, added after 35 min of VF had elapsed, converted the broad FFT spectra during VF to a single frequency. Modified, with permission, from Riccio *et al.* [13].

APD alternans over a wide range of pacing basic cycle lengths (BCL) [33]. Using this model, the L-type Ca^{2+} current was implicated as an important determinant of APD alternans, according to the mechanism shown in Fig. 5. On initiation of pacing at a short BCL, I_{Ca} is fully recovered before the first action potential and activates fully during the action potential, which results in a long APD. The long action potential is subsequently followed by a short diastolic interval, during which I_{Ca} fails to recover completely from Ca^{2+}-induced inactivation. Because of decreased availability of I_{Ca}, the duration of the subsequent action potential is shorter, which results in a longer succeeding diastolic interval, more complete recovery of I_{Ca} and a long action potential duration. This cycle then repeats, eventually establishing a steady-state alternans of I_{Ca} and APD.

Potassium channel agonists and VF

From the mechanism for APD alternans outlined in Fig. 5, we anticipate that shortening of APD during rapid pacing will prolong DI, which, in turn, might provide adequate time for complete recovery of I_{Ca}. If so, reducing the magnitude of APD alternans could be accomplished by increasing outward repolarizing currents, rather than by decreasing I_{Ca}. This idea has been supported by additional computer modeling studies in which APD alternans was suppressed by increasing any one of several outward repolarizing currents [e.g. the rapid (I_{Kr}) and slow (I_{Ks}) components of the delayed rectifier and the inward rectifier (I_{K1})] [33]. Although agonists for these currents are generally not available, it might be possible to modify currents such as I_{Kr} and I_{Ks} by increasing phosphatidyl inositol bisphosphate (PIP2) levels [34] or by altering the phosphorylation state of the channels [35–37], provided the channels can be phosphorylated without concomitant phosphorylation of calcium channels or can be upregulated

in the presence of a calcium channel antagonist, to offset increased I_{Ca} secondary to phosphorylation [38].

Recently, we have focused on increasing I_{Kr} as an approach to suppressing APD alternans. I_{Kr} has an important role in cardiac repolarization, increasing to a maximum during phase three of the action potential, as the channel recovers from inactivation, and then decreasing as the electrical driving force decreases and as deactivation of the channel increases [39–43]. Because I_{Kr} contributes minimally to the action potential plateau, increasing I_{Kr} can have little or no effect on the Ca^{2+} transient. Consequently, by increasing I_{Kr} it can be possible to suppress APD alternans without adversely affecting contractility.

At present, however, there are no I_{Kr} agonists available to test this hypothesis. To circumvent this problem, we infected isolated ventricular myocytes with an adenovirus expressing HERG, the gene that encodes the pore-forming domain of I_{Kr}, to increase HERG protein expression level and the corresponding I_{Kr} current [44] [Hua, F. *et al.*, unpublished data]. After verifying that I_{Kr} had increased post-infection, the myocytes were paced at rapid rates to determine whether increasing I_{Kr} by overexpressing HERG suppressed APD alternans. As shown in Fig. 6, overexpression of HERG markedly increased I_{Kr}, as recorded during action potential clamp, and suppressed APD alternans during rapid pacing. Overexpression of HERG did not, however, significantly reduce I_{Ca}, suggesting that this approach to suppression of alternans need not be accompanied by a reduction in contractility.

The current paradigm regarding I_{Kr} and VF is that blocking I_{Kr} is expected to be anti-arrhythmic, secondary to prolongation of APD and refractoriness [45,46]. However, this approach has not been successful in preventing VF and, moreover, is associated with pro-arrhythmia [45]. Prolongation of APD, as reflected by an increased duration of the QT interval on the ECG, and an increase in the incidence of ventricular arrhythmias are also associated with the administration of numerous non-cardiac drugs that block I_{Kr} [47–50]. Similarly, inherited loss-of-function mutations in I_{Kr} are accompanied by a prolongation of the QT interval and by an increased risk of lethal ventricular tachyarrhythmias, such as *torsade de pointes* [51–54].

The cardiac arrhythmias associated with inherited or drug-induced abnormalities of I_{Kr} are thought to be precipitated primarily by bradycardia-induced prolongation of repolarization [51,52]. The potential mechanisms by which I_{Kr} might facilitate the induction of arrhythmias at slow heart rates have been studied extensively [46,50,53]. However, the contribution of I_{Kr} to repolarization during tachycardia, which might also be important for the development of cardiac arrhythmias, has not been well

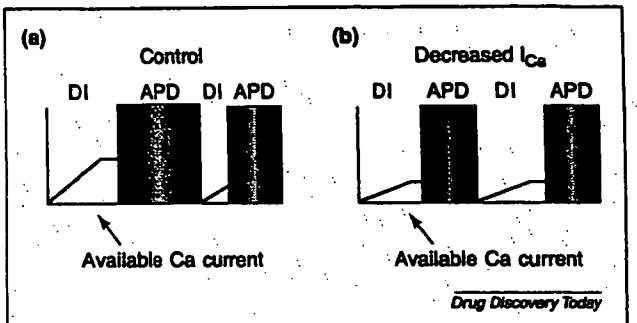

Figure 5. Putative mechanism for action potential duration (APD) alternans and the suppression of alternans by calcium channel blockade. **(a)** Under control conditions, alternation of the length of the diastolic intervals (DI) during APD alternans causes alternation of the magnitude of I_{Ca}, secondary to incomplete recovery of I_{Ca} from inactivation during the short DI. **(b)** Reduction of I_{Ca} decreases APD, which prolongs DI, so that DI following each APD is sufficiently long to enable complete recovery of I_{Ca}. In the absence of alternations of I_{Ca}, APD alternans is suppressed.

characterized. The observation that reducing I_{Kr} increases the magnitude of APD alternans could provide an additional mechanism to account for the proarrhythmic effects of I_{Kr} blockers, in that increased alternans magnitude would be expected to destabilize ventricular tachyarrhythmias, leading to the development of VF. Conversely, the observation that increasing I_{Kr} reduces the magnitude of APD alternans and the slope of the APD restitution relation provides a rationale for the development of a new class of compounds, I_{Kr} agonists, with the expectation that such compounds might have anti-fibrillatory effects.

The latter hypothesis relies, however, on the expectation that I_{Kr} can be increased sufficiently to reduce the slope of the restitution relation without shortening action potential duration to such an extent that contractility is impaired, secondary to a shortening of the plateau duration and attenuation of I_{Ca}. In addition, shortening of APD could lead to a reduction in the wavelength of re-entry circuits (in which wavelength = refractory period × conduction velocity). Reduction of the wavelength could, in turn, precipitate wavebreak by other mechanisms (e.g. so-called 'head–tail' interactions, in which a wavefront encounters a waveback and fragments) [55]. These and other potential drawbacks to the use of K-channel agonists to suppress VF remain to be evaluated critically.

Potential implications for drug development and evaluation

Until recently, therapy for the prevention of sudden cardiac death had been based on the presumption that frequent ventricular ectopy, in particular ventricular tachycardia, is a prelude to ventricular fibrillation [2]. Accordingly, drugs

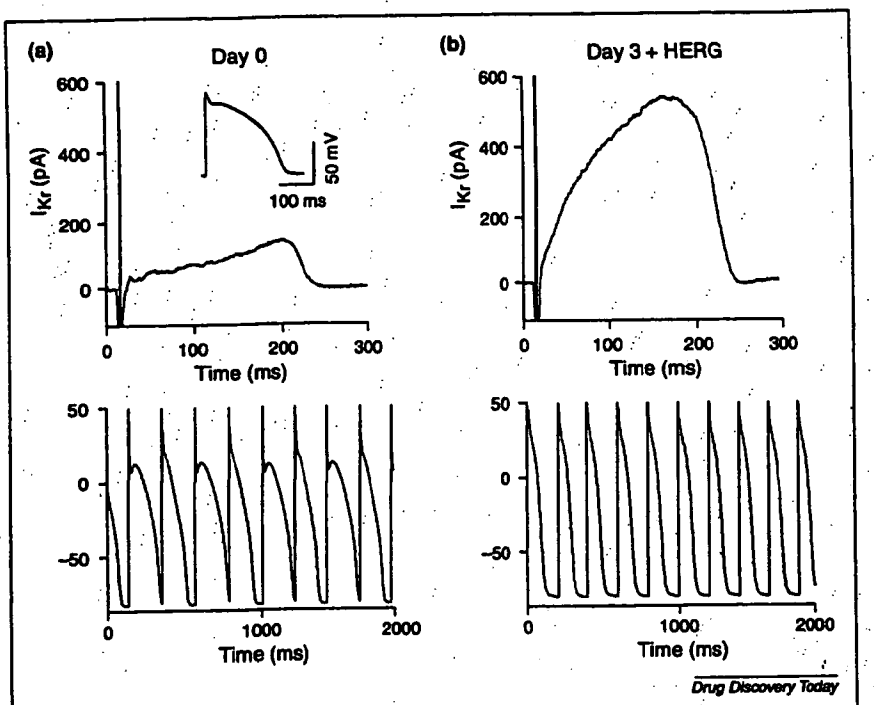

Figure 6. Effects of HERG overexpression on I_{Kr} and action potential duration (APD) alternans in isolated canine cardiac myocytes. (a) Current traces of I_{Kr} (upper panel) and action potentials during pacing at CL = 200 msec (lower panel) obtained from myocytes in the day of isolation (Day 0). (b) Current traces of I_{Kr} (upper panel) and action potentials during pacing at cycle length (CL) = 200 msec (lower panel) obtained from myocytes after three days in cell culture and infection with adenovirus (Day three + HERG). HERG overexpression increased I_{Kr} and suppressed APD alternans.

that suppress inducible or spontaneously occurring ventricular tachycardia are expected to prevent sudden death. However, recent large-scale clinical trials have indicated that classes of drugs that are effective for the suppression of ventricular tachycardia, for example, Class I and Class III antiarrhythmic drugs, do not prevent sudden death and, in fact, could be proarrhythmic [45,56]. In contrast, other classes of drugs that are not particularly effective for the suppression of most forms of ventricular tachycardia, such as β-adrenergic receptor antagonists [57] and calcium channel antagonists [58], could reduce mortality from sudden death.

If a causal relationship between the slope of the APD restitution relation and VF is confirmed, such a result could have significant implications for the pharmacological therapy of sudden cardiac death. Drugs that reduce the slope of the restitution relation would be expected to prevent the development of VF, but would not be expected to suppress ventricular tachycardia, if ventricular tachycardia is caused by some variant of spiral wave re-entry. Conversely, drugs that do not reduce the slope of the restitution relation would not be expected to prevent VF, although they might suppress ventricular tachycardia, perhaps via a mechanism that does not involve alteration of restitution kinetics (e.g. slowing of conduction or prolongation of refractoriness).

Given these expectations, the value of existing agents for the prevention of VF could be re-evaluated in the light of their effects on the restitution relation and new drugs targeted against restitution could be developed. Naturally, such an effort would need to recognize that factors other than APD restitution significantly contribute to the induction and maintenance of VF. Furthermore, drugs intended to alter restitution selectively might have additional effects that could offset their intended effect. Nevertheless, judicious alteration of the APD restitution slope appears to be a promising approach to the treatment of VF and, as such, represents a potentially fruitful opportunity for drug development.

Conclusions

Electrical restitution is a recent addition to factors that play a key role in the development of ventricular tachyarrhythmias. Experimental interventions that reduce the slope of the restitution relation have been effective in suppressing VF. These results encourage further investigation of altering restitution as a means of preventing sudden death, with the realization that clinically useful interventions that flatten restitution without having untoward effects have yet to be developed.

Acknowledgements

I thank Fei Hua, Jeffrey Fox and Mark Riccio for helpful comments and criticisms. This work was supported by grants from the National Institutes of Health, the National Science Foundation and the American Heart Association, New York State Affiliate.

References

1 Zipes, D.P. and Wellens, H.J. (1998) Sudden cardiac death. *Circulation* 98, 2334–2351
2 Myerburg, R.J. *et al.* (1995) Life-threatening ventricular arrythmias: the link between epidemiology and pathophysiology. In *Cardiac Electrophysiology: From Cell to Bedside* (Zipes, D.P. and Jalife, J. eds), pp. 723–731, WB Saunders Co., Philadelphia
3 Krinsky, V.I. and Efimov, I.R. (1992) Vortices with linear cores in mathematical models of excitable media. *Physica A* 188, 55–60
4 Winfree, A.T. (1998) Evolving perspectives during 12 years of electrical turbulence. *Chaos* 8, 1–20

5 Allessie, M.A. *et al.* (1977) Circus movement in rabbit atrial muscle as a mechanism of tachycardia. III. The 'leading circle' concept: a new model of circus movement in cardiac tissue without the involvement of an anatomical obstacle. *Circ. Res.* 41, 9–18

6 Frazier, D.W. *et al.* (1989) Stimulus-induced critical point. Mechanism for electrical initiation of reentry in normal canine myocardium. *J. Clin. Invest.* 83, 1039–1052

7 Witkowski, F.X. *et al.* (1998) Spatiotemporal evolution of ventricular fibrillation. *Nature* 392, 78–82

8 Weiss, J.N. *et al.* (1999) Chaos and the transition to ventricular fibrillation: a new approach to antiarrhythmic drug evaluation. *Circulation* 99, 2819–2826

9 Chen, P.S. *et al.* (1988) Mechanism of ventricular vulnerability to single premature stimuli in open-chest dogs. *Circ. Res.* 62, 1191–1209

10 Gilmour, R.F., Jr and Chialvo, D.R. (1999) Electrical restitution, critical mass, and the riddle of fibrillation. *J. Cardiovasc. Electrophysiol.* 10, 1087–1089

11 Pertsov, A.M. *et al.* (1993) Spiral waves of excitation underlie reentrant activity in isolated cardiac muscle. *Circ. Res.* 72, 631–650

12 Garfinkel, A. *et al.* (2000) Preventing ventricular fibrillation by flattening cardiac restitution. *Proc. Natl. Acad. Sci. U. S. A.* 97, 6061–6066

13 Riccio, M.L. *et al.* (1999) Electrical restitution and spatiotemporal organization during ventricular fibrillation. *Circ. Res.* 84, 955–963

14 Panfilov, A. and Pertsov, A. (2001) Ventricular fibrillation: evolution of the multiple wave hypothesis. *Philos. Trans. R. Soc. Lond. Ser. A.* 359, 1315–1325

15 Fenton, F.H. *et al.* (2002) Multiple mechanisms of spiral wave breakup in a model of cardiac electrical activity. *Chaos* 12, 852–892

16 Karma, A. (1993) Spiral breakup in model equations of action potential propagation in cardiac tissue. *Phys. Rev. Lett.* 71, 1103–1106

17 Karma, A. (1994) Electrical alternans and spiral wave breakup in cardiac tissue. *Chaos* 4, 461–472

18 Moe, G.K. (1964) A computer model of atrial fibrillation. *Am. Heart J.* 67, 200–220

19 Guevara, M.R. *et al.* (1984) Electrical alternans and period doubling bifurcations. *IEEE Comp. Cardiol.* 562, 167–170

20 Chialvo, D.R. *et al.* (1990) Low dimensional chaos in cardiac tissue. *Nature* 343, 653–657

21 Karagueuzian, H.S. *et al.* (1993) Action potential alternans and irregular dynamics in quinidine-intoxicated ventricular muscle cells. Implications for ventricular proarrhythmia. *Circulation* 87, 1661–1672

22 Nolasco, J.B. and Dahlen, R.W. (1968) A graphic method for the study of alternation in cardiac action potentials. *J. Appl. Physiol.* 25, 191–196

23 Rosenbaum, D.S. *et al.* (1994) Electrical alternans and vulnerability to ventricular arrhythmias. *New Engl. J. Med.* 330, 235–241

24 Pastore, J.M. *et al.* (1999) Mechanism linking T-wave alternans to the genesis of cardiac fibrillation. *Circ. Res.* 99, 1385–1394

25 Koller, M.L. *et al.* (1998) Dynamic restitution of action potential duration during electrical alternans and ventricular fibrillation. *Am. J. Physiol.* 275, H1635–H1642

26 Koller, M.L. *et al.* (2000) Effects of $[K^+]_o$ on electrical restitution and activation dynamics during ventricular fibrillation. *Am. J. Physiol. Heart Circ. Physiol.* 279, H2665–H2672

27 Fox, J.J. *et al.* (2002) Spatiotemporal transition to conduction block in canine ventricle. *Circ. Res.* 90, 289–296

28 Chen, P.S. *et al.* (1997) Spirals, chaos, and new mechanisms of wave propagation. *Pacing Clin. Electrophysiol. (PACE)* 20, 414–421

29 Panfilov, A. (1998) Spiral breakup as a model of ventricular fibrillation. *Chaos* 8, 57–64

30 Chudin, E. *et al.* (1999) Intracellular Ca^{2+} dynamics and the stability of ventricular tachycardia. *Biophys. J.* 77, 2930–2941

31 Winslow, R.L. *et al.* (1999) Mechanisms of altered excitation-contraction coupling in canine tachycardia-induced heart failure, II. *Circ. Res.* 84, 571–586

32 Luo, C.H. and Rudy, Y. (1994) A dynamic model of the cardiac ventricular action potential, I: simulation of ionic currents and concentration changes. *Circ. Res.* 74, 1071–1096

33 Fox, J.J. *et al.* (2002) Ionic mechanism of cardiac alternans. *Am. J. Physiol.* 282, H516–H530

34 Bian, J. *et al.* (2001) HERG K^+ channel activity is regulated by changes in phosphatidyl inositol 4,5-bisphosphate. *Circ. Res.* 89, 1168–1176

35 Kiehn, J. (2001) Regulation of the cardiac repolarizing HERG potassium channel by protein kinase A. *Trends Cardiovasc. Med.* 10, 205–209

36 Heath, B.M. and Terrar, D.A. (2000) Protein kinase C enhances the rapidly activated delayed rectifier potassium current, I_{Kr}, through a reduction in C-type inactivation in guinea pig ventricular myocytes. *J. Physiol.* 522, 391–402

37 Marx, S.O. *et al.* (2002) Requirement of a macromolecular signaling complex for β adrenergic receptor modulation of the KCNQ1-KCNE1 potassium channel. *Science* 295, 496–499

38 Reuter, H. and Scholz, H. (1977) The regulation of calcium conductance of cardiac muscle by adrenaline. *J. Physiol.* 246, 49–62

39 Sanguinetti, M.C. and Jurkiewicz, N.K. (1990) Two components of cardiac delayed rectifier K^+ current. Differential sensitivity to block by class III antiarrhythmic agents. *J. Gen. Physiol.* 96, 195–215

40 Rocchetti, M. *et al.* (2001) Rate dependency of delayed rectifier currents during the guinea pig ventricular action potential. *J. Physiol.* 534, 721–732

41 Gintant, G.A. (2000) Characterization and functional consequences of delayed rectifier current transient in ventricular repolarization. *Am. J. Physiol.* 278, H806–H817

42 Gintant, G.A. (1995) Regional differences in I_K density in canine left ventricle: role of I_{Ks} in electrical heterogeneity. *Am. J. Physiol.* 268, H604–H613

43 Clay, J.R. *et al.* (1995) A quantitative description of the E-4031-sensitive repolarization current in rabbit ventricular myocytes. *Biophys. J.* 69, 1830–1837

44 Nuss, H.B. *et al.* (1999) Overexpression of a human potassium channel suppresses cardiac hyperexcitability in rabbit ventricular myocytes. *J. Clin. Invest.* 103, 889–896

45 Waldo, A.L. *et al.* (1996) Effect of d-sotalol on mortality in patients with left ventricular dysfunction after recent and remote myocardial infarction. The SWORD Investigators. Survival with ORal D-sotalol. *Lancet* 348, 7–12

46 Hondeghem, L.M. and Snyders, D.J. (1990) Class III antiarrhythmic agents have a lot of potential but a long way to go. Reduced effectiveness and dangers of reverse use dependence. *Circulation* 81, 686–690

47 Mohammad, S. *et al.* (1997) Blockage of the HERG human cardiac K^+ channel by the gastrointestinal prokinetic agent cisapride. *Am. J. Physiol.* 273, H2534–H2538

48 Roy, M. *et al.* (1996) HERG, a primary human ventricular target of the nonsedating antihistamine terfenadine. *Circulation* 94, 817–823

49 Mitcheson, J.S. *et al.* (2000) A structural basis for drug-induced long QT syndrome. *Proc. Natl. Acad. Sci. U. S. A.* 97, 12329–12333

50 Mitcheson, J.S. *et al.* (2000) A structural basis for drug-induced long QT syndrome. *Proc. Natl. Acad. Sci. U. S. A.* 97, 12329–12333

51 Keating, M.T. and Sanguinetti, M.C. (1996) Molecular genetic insights into cardiovascular disease. *Science* 272, 681–685

52 Curran, M.E. *et al.* (1995) A molecular basis for cardiac arrhythmia: HERG mutations cause long QT syndrome. *Cell* 80, 795–803

53 Roden, D.M. and Balser, J.R. (1999) A plethora of mechanisms in the HERG-related long QT syndrome. Genetics meets electrophysiology. *Cardiovasc. Res.* 44, 242–246

54 Sanguinetti, M.C. *et al.* (1995) A mechanistic link between an inherited and an acquired cardiac arrhythmia: HERG encodes the I_{Kr} potassium channel. *Cell* 81, 299–307

55 Hund, T.J. *et al.* (2000) Dynamics of action potential head–tail interaction during reentry in cardiac tissue: ionic mechanisms. *Am. J. Physiol.* 279, H1869–H1879

56 Echt, D.S. *et al.* (1991) Mortality and morbidity in patients receiving encainide, flecainide or placebo: the cardiac arrhythmia suppression trial. *New Engl. J. Med.* 324, 781–788

57 Yusuf, S. *et al.* (1988) Overview of results of randomized clinical trials in heart disease: I. Treatments following myocardial infarction. *J. Am. Med. Assoc.* 260, 2088–2095

58 Held, P.H. and Yusuf, S. (1994) Impact of calcium channel blockers on mortality. In *Cardiovascular Pharmacology and Therapeutics* (Singh, B.N. *et al.*, eds), pp. 525–533, Churchill Livingston

Dynamic mechanism for conduction block in heart tissue

Abstract. Previous work has shown that dynamic heterogeneity and conduction block can occur in homogeneous heart fibres during prolonged pacing at rapid rates. Here we investigated the mechanism for conduction block following the delivery of one to four premature stimuli using a coupled maps computer model of a one-dimensional canine heart fibre. The coupled maps model allowed us to identify the roles that velocity (V) restitution, action potential duration (D) restitution and cardiac memory (M) played in the development of spatial heterogeneity and conduction block. We found that the likelihood of conduction block could be reduced by three methods. (1) By altering the V restitution function so that conduction slowed at very short rest intervals (I). (2) By altering the D restitution function to reduce the sensitivity of D to changes in I. (3) By increasing the contribution of cardiac memory (M). Although the results of this study need to be confirmed experimentally, they suggest several potential interventions that may reduce the probability of arrhythmia induction.

101.2

C ntents

1. Introduction

Catastrophic heart rhythm disorders are among the leading causes of death in the United States. The most dangerous of these arrhythmias is ventricular fibrillation, a disturbance in which disordered wave propagation causes a fatal disruption of the synchronous contraction of the ventricle. Although the exact mechanism for fibrillation is still being debated, one theory proposes that fibrillation is a state of spatiotemporal chaos consisting of the perpetual nucleation and disintegration of spiral waves [4, 26], in association with a period doubling bifurcation of local electrical properties [13, 14, 16, 18]. Nucleation of the initiating spiral wave pair is caused by local conduction block (wave break) secondary to spatial heterogeneity of refractoriness in the ventricle [2, 4, 22, 25, 26]. Until recently, spatial heterogeneity was thought to result solely from regional variations of intrinsic cellular electrical properties [22, 27] or from stimulation at more than one spatial location [20, 24, 25]. However, it is now appreciated that purely dynamical heterogeneity can be sufficient to cause conduction block during single-site stimulation in both homogeneous one-dimensional models of canine heart tissue and in rapidly paced canine Purkinje fibres [8, 12]. A similar mechanism has been shown to precipitate conduction block and spiral break-up in models of homogeneous two-dimensional tissue [9].

The period doubling bifurcation implicated in the transition to conduction block is manifest as alternans, a beat-to-beat long–short alternation in the duration of the cardiac action potential [13, 14, 16, 18, 24]. Previous investigators have hypothesized that alternans can be accounted for by a simple uni-dimensional return map called the action potential duration restitution function [5, 6, 15, 17]. This hypothesis assumes the duration D of an action potential depends only on its preceding rest interval I through some function $f(I)$ that is measured experimentally. If the D restitution function has a slope ≥ 1, then a period doubling bifurcation occurs for some value of the stimulus period T, where $T = D + I$. The velocity V at which an action potential propagates can also be described by a restitution function, where $V = c(I)$.

It has been shown previously that the combination of a steeply sloped D restitution function and a monotonically increasing V restitution function is sufficient to produce dynamical conduction block during sustained pacing at a short cycle length [11, 12]. This observation may provide a generic mechanism for wave break and the onset of ventricular tachycardia and

fibrillation. However, it is unlikely that the conditions used to demonstrate this phenomenon experimentally apply to the clinical situation, where the induction of ventricular tachyarrhythmias is typically associated with the interruption of normal cardiac rhythm by only a few premature beats. A single premature beat is sufficient to cause spatial heterogeneity in the form of discordant alternans [24], but the conditions required for the development of conduction block in this setting have not been investigated.

To address this issue, in the present study we determined whether dynamic heterogeneity and conduction block occur in a computer model of canine heart fibres in which pacing at a slow rate is interrupted by one to four premature stimuli. This protocol simulates the interruption of sinus rhythm by one to four premature ventricular complexes (PVCs), a situation that can lead to the onset of ventricular fibrillation clinically. Furthermore, we determined whether such conduction block can be accounted for by the same dynamical mechanism that underlies the development of conduction block during rapid pacing. A coupled maps model of heart tissue was used for the study, which allowed us to identify the roles that V and D restitution play in the development of dynamic heterogeneity. We also considered the additional contribution of cardiac memory (M) to the development of dynamical heterogeneity and conduction block.

2. Methods

We studied the mechanism for conduction block following the delivery of multiple premature stimuli using a one-dimensional computer model of a canine heart fibre. The length of the fibre was 4 cm, which is similar to the length of fibres used for previous experimental studies [12]. The fibre was stimulated at one end at a cycle length near normal canine sinus rhythm (S1 = 500 ms). After ten beats at S1, four premature stimuli were delivered (S2, S3, S4 and S5) at the same site. The coupling intervals between these premature intervals were varied and the conduction of the resultant action potentials was observed (figure 1). For each combination of premature stimuli, one of three possible outcomes occurred:

(1) the stimulus elicited an action potential that propagated down the entire fibre;

(2) the stimulus did not produce an action potential (type I block);

(3) the stimulus elicited an action potential that blocked before reaching the end of the fibre (type II block).

The first two cases would not be conducive to the development of wave break and initiation of re-entry, in that conduction of the premature response either does not occur at all or occurs equally well everywhere along the fibre. The third case, however, could lead to wave break and spiral wave initiation if it occurred in two- and three-dimensional tissue, provided the block was local. The development of local block would be facilitated in intact myocardium by twist anisotropy and intrinsic heterogeneity.

To assess the vulnerability of the simulated tissue to type II block, the S2–S3–S4–S5 combinations were applied in the following way: the S1–S2 interval was varied from the minimum value that conducted (S1–$S2_{min}$) to S1–$S2_{min}$ + 20 ms. For each S1–S2 interval, the S2–S3 interval and the S3–S4 interval were varied in combination from the minimum value that conducted up to a value of 250 ms for each interval. Finally, for each S2–S3–S4 combination that conducted, the S4–S5 interval was varied from the minimum that generated an action potential at the site of stimulation to the minimum value that conducted down the entire fibre. If no

101.4

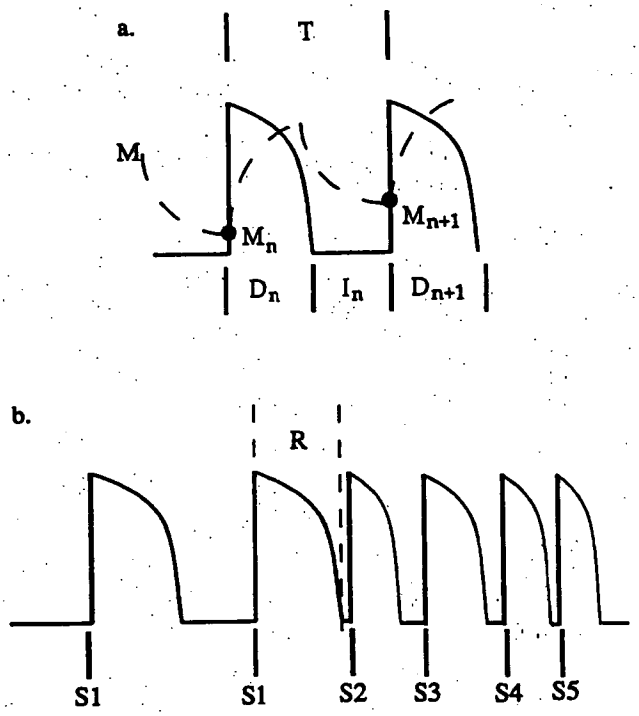

Figure 1. (a) Schematic representation of the relationships between stimulus period (T), action potential duration (D), diastolic interval (I) and memory (M). (b) Example of the stimulation protocol. The model fibre was paced for ten beats at a constant S1–S1 interval, after which a series of premature stimuli (S2–S5) was delivered. R indicates the refractory period of a cardiac cell, during which the delivery of a stimulus does not produce a propagated response.

S2–S3–S4–S5 combination was found that produced conduction block for more than a 20 ms window in either the S2–S3 interval or the S3–S4 interval, the search was halted for that interval. All intervals were varied in steps of 1 ms.

2.1. *Coupled maps model*

The study was conducted using a coupled maps model of a one-dimensional cardiac fibre that has been described in detail elsewhere [10, 12]. Briefly, the model is based on the equation

$$I_{n+1}(x_i) = T_{n+1}(x_i) - D_{n+1}(x_i). \tag{1}$$

$T_{n+1}(x_i)$ was the time interval between activations of site x_i. It was determined by including the time delays caused by the propagation from the pacing site to site x_i, which yielded

$$T_{n+1}(x_i) = \tau + \sum_{j=0}^{i-1} \frac{\Delta x}{V_{n+1}(x_j)} - \sum_{j=0}^{i-1} \frac{\Delta x}{V_n(x_j)}. \tag{2}$$

τ was the time interval between activations applied to the pacing site and $\Delta x = 0.1$ was the length of a single cell (time units in milliseconds and space units in millimetres). The conduction

velocity $V_n(x_i)$ depended only on I through the velocity recovery function $V_n = c(I_n)$ given by $c(I) = V_{max}(1 - \exp(-(I + \beta)/\delta))$. $V_{max} = 0.72$, $\delta = 14$, and β was varied to adjust the value of V at $I = I_{min}$. D was determined locally based on a memory model mapping [10] given by

$$\begin{aligned} M_{n+1} &= g(M_n, I_n, D_n) = e^{-I_n/\tau_m}[1 + (M_n - 1)e^{-D_n/\tau_m}] \\ D_{n+1} &= f(M_{n+1}, I_n) = (1 - \alpha M_{n+1})\left(A + \frac{B}{1 + e^{-(I_n - C)/\tau_D}}\right). \end{aligned} \tag{3}$$

τ_m was the time constant of accumulation and dissipation of memory (both constants were chosen to be the same). $A = 88$, $B = 122$, $C = 40$ and $\tau_m = 180$ [10]. α and τ_D were varied in this study. α (which varied between zero and unity) determined the influence of memory on D, and τ_D was used to adjust the dependence of the D recovery function on I. We note that, for memory models, the dependence of D on I (as well as the occurrence of a period doubling bifurcation) is not related to the steady-state restitution slope in a simple manner [10].

Coupling between sites was included by using the diffusion terms from Echebarria and Karma [8]. These terms modelled the electrotonic current that flowed out of (into) a cell and into (out of) its neighbour if the action potential of the first cell was longer (shorter) than that of its neighbour. Including diffusion then yielded

$$D_{n+1} = f(M_{n+1}, I_n) + \xi^2 \nabla^2 D_{n+1} - w \nabla D_{n+1}, \tag{4}$$

with $\xi = 1.0$ and $w = 0.35$. Discretizing the derivatives produced a tri-diagonal linear system of equations that could then be solved easily. The defining equation for the model was therefore

$$\begin{aligned} M_{n+1} &= g(M_n, I_n, D_n) \\ D_{n+1} &= f(M_{n+1}, I_n) + \xi^2 \nabla^2 D_{n+1} - w \nabla D_{n+1} \\ I_{n+1}(x_i) &= \tau + \sum_{j=0}^{i-1} \frac{\Delta x}{c(I_{n+1}(x_j))} - \sum_{j=0}^{i-1} \frac{\Delta x}{c(I_n(x_j))} - D_{n+1}(x_i). \end{aligned} \tag{5}$$

Finally, conduction block was modelled by setting $f = 0$ for $I < I_{min} = 2$.

3. Results

3.1. Characteristics of conduction block in the wild type model

Figure 2 shows a typical example of type II conduction block in the baseline model (hereafter called the wild type model). Despite the homogeneous state that existed at the end of the S1 stimuli, dynamical heterogeneity developed following delivery of S2, secondary to V restitution (see below). Heterogeneity was manifest as a short-to-long gradient in I, which was magnified by subsequent premature stimuli until the action potential generated by the S5 stimulus encountered a region where $I < I_{min}$ and conduction failed.

Figure 3 shows a histogram of type II conduction block at various S2 and S3 intervals generated from the wild type model. Note the presence of a large peak centred at an S2 very close to the minimum value for conduction and at an S3 approximately 50 ms longer than the minimum value for conduction. Surrounding the peak is a flat plateau region of five to ten blocks per bin that extends throughout the entire (S2, S3) region that was explored numerically. An overwhelming majority of these instances of block occurred after the S5 stimulus. However, six examples of 'early block' were found after an S4 stimulus, and one was found after an S3

101.6

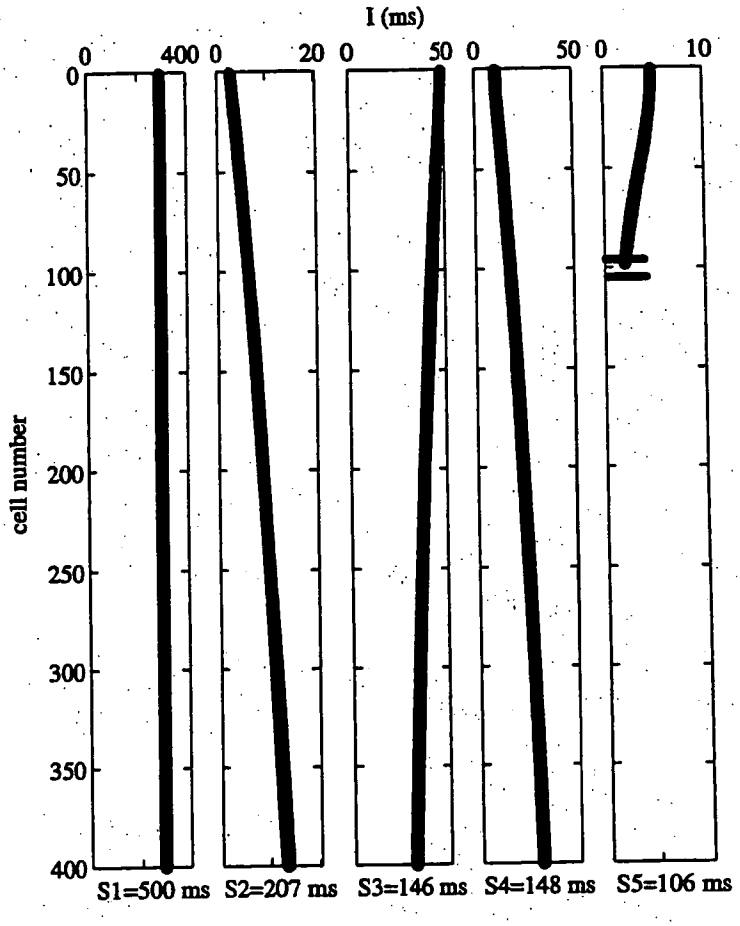

Figure 2. Example of type II conduction block in the coupled maps model. Each panel shows I as a function of cell number for the last S1 = 500 ms beat (left panel) and for beats S2 = 207 ms, S3 = 146 ms, S4 = 148 ms and S5 = 106 ms. Note the difference in scale for each beat. Conduction block, corresponding to $I < I_{min}$, occurs near cell 100 on the S5 beat and is denoted by two horizontal black lines.

stimulus. The latter explain the presence of the plateau in the histogram; the plateau is made up of 'degenerate' counts in which long S2 or S3 intervals that maintained the initial S1 homogeneity were followed by early block intervals leading to block at S5.

Since conduction block occurs when $I < I_{min}$, changes in I_{min} will produce significant changes in the incidence of conduction block. Because I_{min} is a component of the functions that control V restitution, D restitution and M, changes in I_{min} influence all three dynamic variables. In this study, we held I_{min} fixed and individually studied the roles that V restitution, D restitution and M played in determining the risk of type II block, as assessed by the S2–S3–S4–S5 protocol.

3.2. Contribution of V restitution to conduction block

V restitution played two important roles in the development of conduction block. First, as mentioned above, V restitution was the source of the initial heterogeneity after delivery of the

101.7

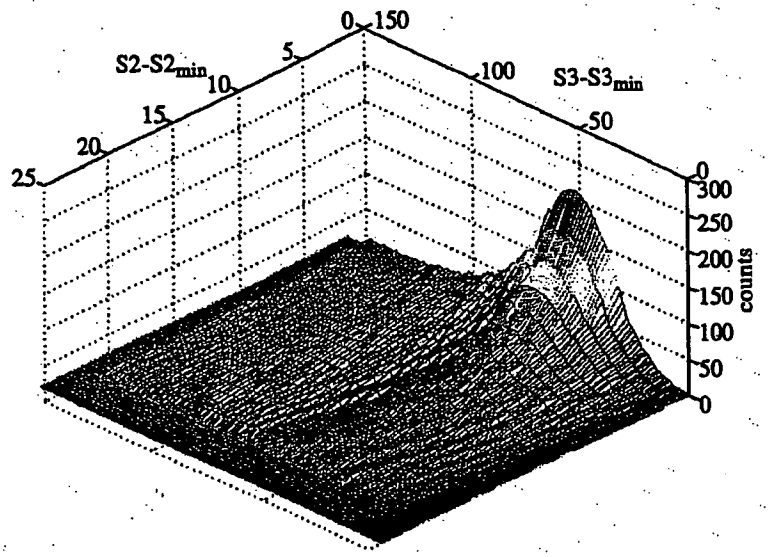

Figure 3. Histogram of the incidence of type II conduction block in the wild type model. $\alpha = 0.2$, $\tau_D = 28$ and $\beta = 17.408$. The height at each point in (S2, S3) space corresponds to the number of blocks found at beat S3, S4 or S5 for a given (S2, S3) pair. $S2_{min}$ and $S3_{min}$ are as defined in the methods section. Total counts = 67 205.

S2 stimulus. The S2 stimulus was delivered just after the refractory period of the last S1 beat so that I at the site of stimulation was short (see figure 1). The short I produced slow V, which increased I for cells distal to the stimulus site. This initial dispersion in I following S2 was magnified by steep D restitution at each subsequent beat, ultimately leading to conduction block several beats later.

Second, the value of the V restitution curve at I_{min} was an important parameter in determining the likelihood of conduction block, as illustrated by figure 4. Panel (a) shows V restitution curves with four different values for the $V(I_{min})$ (90, 75, 50, and 25% of V_{max}). $V(I_{min})$ in the wild type model was 75% of V_{max}. Panel (b) shows a histogram for $V(I_{min}) = 50\%$ of V_{max} and panel (c) shows the histogram for $V(I_{min}) = 90\%$ of V_{max}. For $V(I_{min}) = 90\%$ of V_{max}, the model had roughly 30% more instances of conduction block than in the wild type model, whereas the model with the lower cut-off values produced dramatically fewer instances of conduction block. In fact, the model with $V(I_{min}) = 25\%$ of V_{max} produced no cases of type II block. This result did not depend on the steepness of the V restitution curve. For example, no cases of type II block were found for a model with $\beta = -1.4$ and $\delta = 2.0$, which also had $V(I_{min}) = 25\%$ of V_{max}, but had a much steeper slope. The lack of type II block when $V(I_{min}) = 25\%$ of V_{max} can be understood by noting that if the V restitution curve approaches zero at I_{min}, then a propagating wave that approaches a region with a very small I can slow down to allow I to increase just in front of it, permitting continued conduction.

3.3. Contribution of D restitution to conduction block

As mentioned above, D restitution contributed to conduction block by magnifying heterogeneity in I. If the D restitution function had weak dependence on I, any initial dispersion of I due to V

101.8

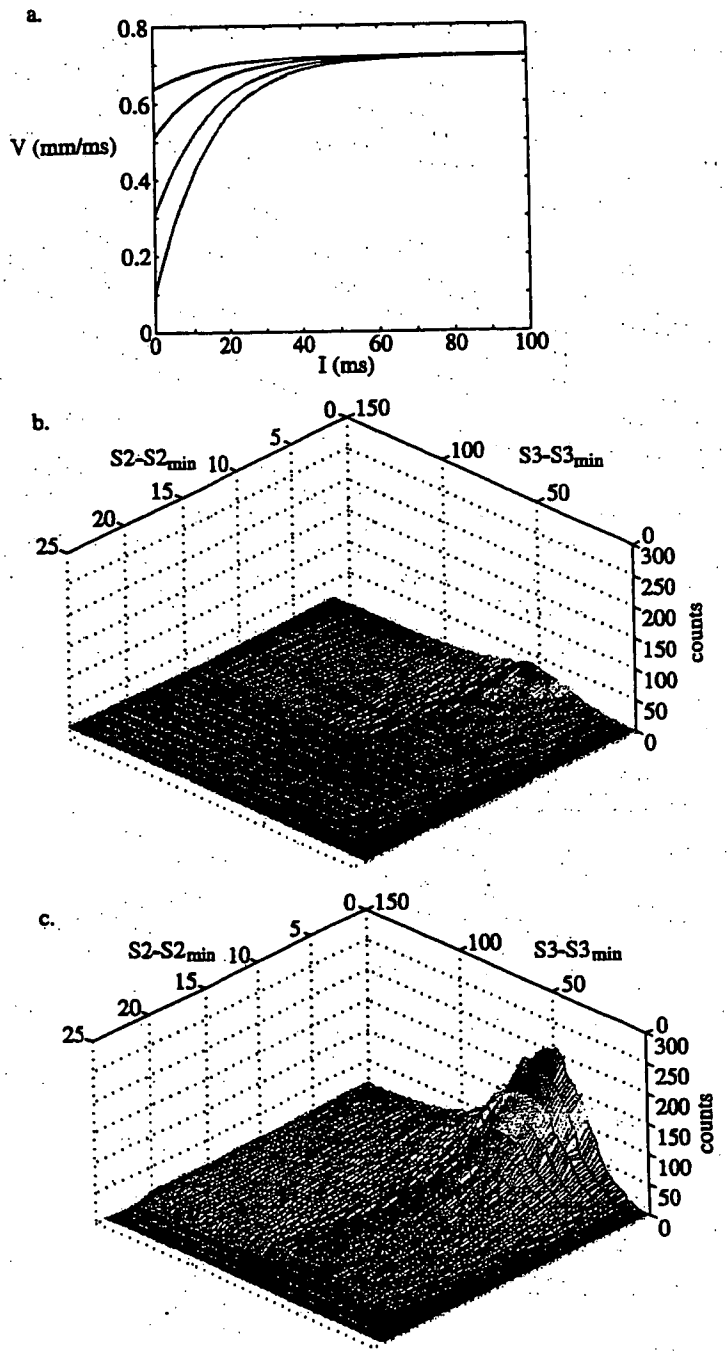

Figure 4. The role of V restitution in type II block. (a) V restitution for four cases: $\beta = 17.408$ (black; wild type), $\beta = 7.704$ (red; $V(I_{min}) = 50\%$ of V_{max}), $\beta = 2.028$ (green; $V(I_{min}) = 25\%$ of V_{max}) and $\beta = 30.236$ (blue; $V(I_{min}) = 90\%$ of V_{max}). (b) Histogram for $V(I_{min}) = 50\%$ of V_{max}. Total counts = 8879 (cf 67 205 for wild type). (c) Histogram for $V(I_{min}) = 90\%$ of V_{max}. Total counts = 86 032. There were no counts for $V(I_{min}) = 25\%$ of V_{max}.

101.9

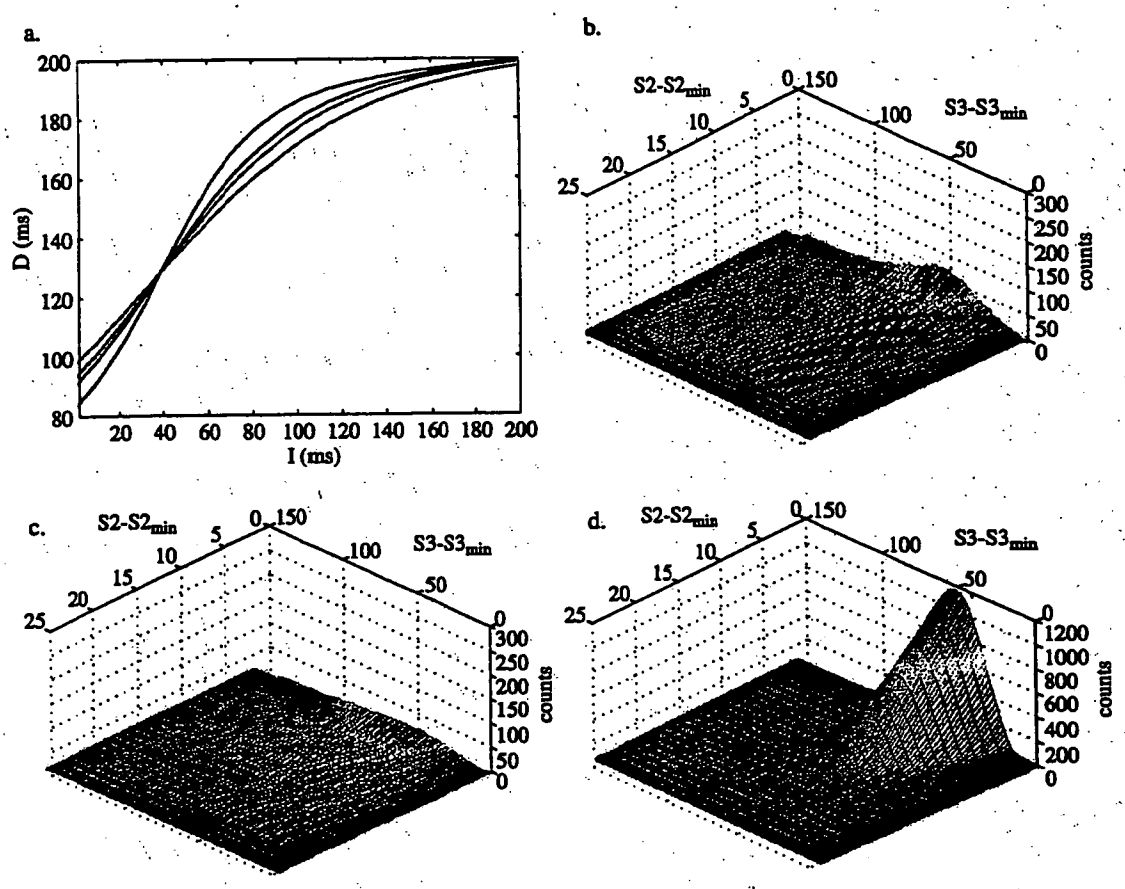

Figure 5. The role of D restitution in type II block. (a) Steady-state D restitution for four cases: $\tau_D = 28$ (black; wild type; max. slope = 1.09), $\tau_D = 32$ (red; max. slope = 0.97), $\tau_D = 40$ (green; max. slope = 0.82) and $\tau_D = 20$ (blue; max. slope = 1.45). (b) Histogram for $\tau_D = 32$. Total counts = 39 688. (c) Histogram for $\tau_D = 40$. Total counts = 21 185. (d) Histogram for $\tau_D = 20$. Total counts = 364 301.

restitution would be lessened on subsequent stimulations. Figure 5 shows the effect of altering D restitution slope by increasing and decreasing the parameter τ_D. Panel (a) shows steady state restitution curves for four different values of τ_D. The wild type model was $\tau_D = 28$. As shown in panels (b) and (c), increasing τ_D led to a significantly smaller peak in the histogram, as well as fewer total instances of conduction block. Conversely, decreasing τ_D, which led to a steeper steady state restitution slope, had significantly more counts (panel (d)). However, it is important to note that even for the $\tau_D = 40$ model, which had a maximum steady state slope of 0.82, instances of type II block were found.

3.4. Contribution of M to conduction block

Because increasing M in the coupled maps model has been shown to eliminate steady state alternans, it was hypothesized that increasing M also would lead to fewer instances of type II block. Figure 6 illustrates the effect of changing M on the likelihood of conduction block in the

model by increasing and decreasing the parameter α. Panel (a) shows steady-state restitution for four different values of α. The wild type model was $\alpha = 0.2$. In panel (b) $\alpha = 0.58$, which eliminated alternans but maintained a slope ≥ 1. In fact, the steady state restitution slope was 1.62, even larger than in the wild type model. In panel (c) $\alpha = 0.8$ and the maximum steady state restitution slope was 2.65. Both panels (b) and (c) show smaller peaks and fewer total counts than the wild type model. In panel (d) M was decreased ($\alpha = 0.1$) and the maximum steady state slope is 1.09. The decreased memory model shows more instances of conduction block than the wild type model. This result did not depend on the magnitude of D. For example, shifting the curve from panel (c) by adding 70 ms to the function $f(M_{n+1}, I_n)$ did not produce more instances of type II block (in fact slightly fewer (39 229) were found). Similarly, shifting the curve from panel (d) down by subtracting 70 ms from $f(M_{n+1}, I_n)$ produced roughly the same number of blocks (94 151) as in panel (d). Two other observations can be made. First, increasing M did not seem to be as effective as increasing τ_D in reducing the likelihood of block. Second, the steady-state D restitution function is not predictive of the likelihood of block.

3.5. Contribution of electrotonic interactions to conduction block

Electrotonic effects have been shown to prevent alternans in some models [7]. Therefore, changes in electrotonic current may be expected to have an effect on the incidence of conduction block. The coupled maps model allowed for the complete removal of electrotonic interactions by eliminating the diffusion terms in equation (4). As shown in figure 2, the potential for conduction block was present when the previous beat generated a short-to-long pattern in I. This pattern led to a short-to-long pattern in the following D. In the wild type model, both the first and second derivative diffusion terms tended to decrease the long D and increase the short D, reducing the amount of heterogeneity and thereby reducing the likelihood of type II block. Accordingly, elimination of the diffusion terms was expected to increase the incidence of type II block and this expectation was confirmed; total counts of type II block were 88 603 (histogram not shown).

4. Discussion

In this study type II conduction block following the delivery of multiple premature stimuli was caused by the same sequence of events that caused conduction block during sustained rapid pacing in our previous study [12]. Stimulation at a short I produced a gradient of increasing I (and, consequently, of D and V) along the fibre. The succeeding stimulus, if delivered at an appropriate interval, encountered a progressively decreasing I as it propagated down the fibre (i.e., the new wavefront encountered the waveback of the previous excitation). Thus, a short–long sequence of D at the site of stimulation was associated with the development of a long–short sequence of D at the opposite end of the fibre, similar to the pattern established during stable discordant alternans [19, 20, 24]. When the gradient in I along the fibre was sufficiently steep in the ascending direction, the subsequent action potential encountered an $I < I_{min}$ and conduction block occurred.

Previous studies have shown that the location of the block can be predicted, given the spatial profile of D for the preceding beat [22]. If this information is not known, however, then developing a quantitative theory for the type II block observed in this study becomes difficult, not only because the model consists of complicated nonlinear difference equations in both space and time, but also because the phenomenon of interest is a transient. Therefore, the usual

101.11

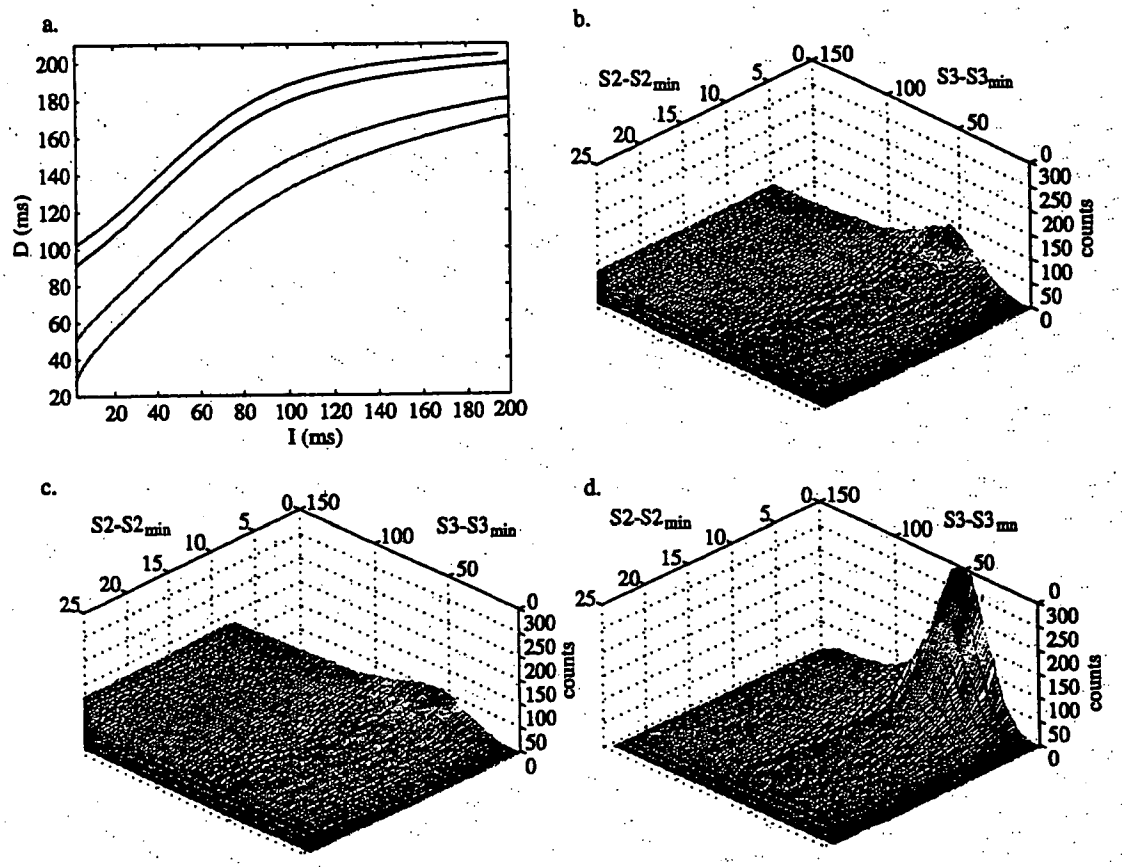

Figure 6. The role of M in type II block. (a) Steady-state D restitution for four cases: $\alpha = 0.2$ (black; wild type; max. slope = 1.09), $\alpha = 0.58$ (red; max. slope = 1.62), $\alpha = 0.8$ (green; max. slope = 2.65) and $\alpha = 0.1$ (blue; max. slope = 1.09). (b) Histogram for $\alpha = 0.58$. Total counts = 48 387. (c) Histogram for $\alpha = 0.8$. Total counts = 43 715. (d) Histogram for $\alpha = 0.1$. Total counts = 87 433.

tools of nonlinear dynamics, such as finding steady-state solutions and analysing their stability, do not apply. Still, inspection of the defining equations produces a qualitative understanding of the results presented in this study. The mechanism for conduction block relies on three determinants. First, a non-constant V restitution function produces spatial heterogeneity in I. Next, this heterogeneity is amplified (or at least it does not decay rapidly) due to sensitive dependence of D on I. Finally, the V restitution function does not drop sufficiently close to zero at very short I, causing the wave to collide with the refractory period of the preceding excitation.

Preventing the first aspect of type II block could only be done by forcing the V restitution curve to be constant. Even in that case, type II block could still occur if there were intrinsic heterogeneity in the fibre. Therefore, we explored how the likelihood of type II block could be diminished by two different methods. The first method was to alter the V restitution function so that conduction slowed at very short I, thus preventing encroachment on the refractory period. It is important to note that this method is only viable if the decrease in conduction velocity occurs at

short I. Decreasing maximum conduction velocity is in fact pro-arrhythmic, because it decreases the wavelength [9]. Although selective slowing of conduction at short rest intervals may create a greater dispersion of refractoriness after a premature beat, the benefits of this intervention seem to outweigh the risks, at least under the conditions of this study. Whether a similar strategy will suppress conduction block in 2D or 3D tissue with realistic intrinsic heterogeneity remains to be determined.

The second method for reducing the likelihood of type II block was to reduce the sensitivity of D on I. If the system is uni-dimensional, this is done by decreasing the D restitution slope. The lower the slope of the D restitution relation, the lower the likelihood of spatial dispersion of repolarization secondary to dispersion of I. However, the model used in this study did not have a simple relationship between the slope of the steady-state D restitution function and the likelihood of block. Instead, the important quantity is the sensitivity of D to the preceding I, given by

$$\gamma = \frac{\mathrm{d}f}{\mathrm{d}I} = \frac{\partial f}{\partial I} + \frac{\partial f}{\partial M}\frac{\partial g}{\partial I}. \tag{6}$$

The quantity γ is the amplification factor relating the dispersion in D to the dispersion in the preceding I. If γ is small, then any initial dispersion in I will decay quickly. If γ is large, the dispersion of I can persist or even be amplified. It can be shown that at short cycle lengths the first term dominates, giving

$$\gamma \approx \frac{\partial f}{\partial I} = (1 - \alpha M^*)\frac{B}{\tau_D}\frac{\mathrm{e}^{-(I^*-C)/\tau_D}}{(1+\mathrm{e}^{-(I^*-C)/\tau_D})^2}. \tag{7}$$

M^* and I^* are the steady state values at a given cycle length. This equation is of limited quantitative use since the system never reaches steady state (and the cycle length is continuously changing). Still, it suggests that the likelihood of block can be reduced by either increasing τ_D or by increasing α. The simulation results support this qualitative argument. This result highlights the fact that the dynamics during premature stimulation cannot be predicted from the steady-state D restitution function. In fact, the more relevant experimental measure would be the S1–S2 D restitution function at very short S2. The slope of this curve at short I would directly measure the dispersion of D after a very short S1–S2 interval had produced some initial dispersion in I. However, relating the S1–S2 curve to any quantitative prediction about type II block is not straightforward.

Programmed electrical stimulation has been used extensively in the past to induce ventricular arrhythmias in patients thought to be at risk for the development of ventricular fibrillation [1]. However, the stimulation protocol used in the clinical studies differs significantly from that used here, in that arrhythmia induction was attempted using tightly coupled premature stimuli, which produced block similar to the type I block described in our study. Once the patient's arrhythmia had been induced using multiple premature stimuli, the test was repeated after administration of an antiarrhythmic drug. In many cases a drug could be found that would suppress the patient's inducible arrhythmia. Yet the results of large scale clinical trials eventually revealed that patients sent home on such medications were as or more likely to die suddenly than patients who did not receive such treatment [3, 23]. Clearly, the induction of arrhythmias using this particular stimulation protocol was not predictive of the development of ventricular fibrillation.

The failure of the standard method of programmed stimulation to accurately assess vulnerability to ventricular fibrillation may relate to the fact that this method was designed

primarily to induce conduction block and re-entry by perturbing intrinsic heterogeneity. The potential contribution of dynamic heterogeneity to the development of conduction block would not be assessed adequately using such a protocol. In addition, interventions that were intended to prevent the induction of arrhythmias using the standard protocol, such as slowing of conduction or prolongation of refractoriness, might be effective in that regard, secondary to a reduction in intrinsic heterogeneity, but might not reduce dynamic heterogeneity. Consequently, the beneficial effects of such interventions on arrhythmias induced by the standard stimulation protocol might not correspond to a reduction in the incidence of ventricular fibrillation, if induction of the latter is influenced importantly by dynamic heterogeneity.

Dynamically induced heterogeneity and conduction block is one of many potential mechanisms for spiral break-up in cardiac tissue (see for example [9]). Because wave propagation in the heart is extremely complex and influenced by many factors, it is unlikely that only one mechanism is responsible for induction and maintenance of all cardiac arrhythmias. Nevertheless, the results of this study suggest several potential interventions that may reduce the probability of arrhythmia induction, including flattening the D restitution slope, decreasing V at short I and increasing M. There is experimental support for the idea that flattening D restitution suppresses ventricular fibrillation [21], but altering V and M with the objective of preventing ventricular fibrillation has not been attempted. Tests of these options may not be likely in the near future, however, given that drugs that increase the recovery of sodium channels at depolarized potentials are not, to our knowledge, currently available, and alteration of M may not be possible until the ionic basis for this phenomenon has been established. Nevertheless, judicious alterations of D, V and M may hold future promise for new and more effective therapies for ventricular fibrillation.

Acknowledgments

These studies were supported by NIH grant no HL62543 (RFG) and by an IGERT training grant from the National Science Foundation (JJF).

References

[1] Anderson K P and Mason J W 1995 Clinical value of cardiac electrophysiology studies *Cardiac Electrophysiology. From Cell to Bedside* 2nd edn, ed D P Zipes and J Jalife (Philadelphia, PA: Saunders) pp 1133–50

[2] Arce H, Xu A X, Gonzalez H and Guevara M R 2000 Alternans and higher-order rhythms in an ionic model of a sheet of ischemic ventricular muscle *Chaos* **10** 411–26

[3] CAST 1989 Preliminary report: effect of encainide and flecainide on mortality in a randomized trial of arrhythmia suppression after a myocardial infarction *New Engl. J. Med.* **321** 406–12

[4] Chen P S, Wolf P D, Dixon E G, Danieley N D, Frazier D W, Smith W M and Ideker R E 1988 Mechanism of ventricular vulnerability to single premature stimuli in open-chest dogs *Circ. Res.* **62** 1191–209

[5] Chialvo D R, Gilmour R F Jr and Jalife J 1990 Low dimensional chaos in cardiac tissue *Nature* **343** 653–7

[6] Chialvo D R and Jalife J 1987 Non-linear dynamics of cardiac excitation and impulse propagation *Nature* **330** 749–52

[7] Cytrynbaum E and Keener J P 2002 Stability conditions for the traveling pulse: modifying the restitution hypothesis *Chaos* **12** 788–99

[8] Echebarria B and Karma A 2002 Instability and spati temporal dynamics f alternans in paced cardiac tissue *Phys. Rev. Lett.* **88** 208101

[9] Fenton F H, Cherry E M, Hastings H M and Evans S J 2002 Multiple mechanisms f spiral wave breakup in a model of cardiac lectrical activity *Chaos* **12** 852–92

[10] Fox J J, Bodenschatz E and Gilmour R F Jr 2002 Period-doubling instability and memory in cardiac tissu *Phys. Rev. Lett.* **89** 138101

[11] Fox J J, Gilmour R F and Bodenschatz E 2002 Conduction block in one-dimensional heart fibers *Phys. Rev. Lett.* **89** 198101

[12] Fox J J, Riccio M L, Hua F, Bodenschatz E and Gilmour R F Jr 2002 Spatiotemporal transition to conduction block in canine ventricle *Circ. Res.* **90** 289–96

[13] Garfinkel A, Kim Y H, Voroshilovsky O, Qu Z, Kil J R, Lee M H, Karagueuzian H S, Weiss J N and Chen P S 2000 Preventing ventricular fibrillation by flattening cardiac restitution *Proc. Natl Acad. Sci. USA* **97** 6061–6

[14] Gilmour R F Jr and Chialvo D R 1999 Electrical restitution, critical mass, and the riddle of fibrillation *J. Cardiovasc. Electrophysiol.* **10** 1087–9

[15] Guevara M R, Ward G, Shrier A and Glass L 1984 Electrical alternans and period doubling bifurcations *IEEE Comput. Cardiol.* **562** 167–70

[16] Karma A 1994 Electrical alternans and spiral wave breakup in cardiac tissue *Chaos* **4** 461–72

[17] Nolasco J B and Dahlen R W 1968 A graphic method for the study of alternation in cardiac action potentials *J. Appl. Physiol.* **25** 191–6

[18] Panfilov A 1998 Spiral breakup as a model of ventricular fibration *Chaos* **8** 57–64

[19] Pastore J M, Girouard S D, Laurita K R, Akar F G and Rosenbaum D S 1999 Mechanism linking T-wave alternans to the genesis of cardiac fibrillation *Circulation* **99** 1385–94

[20] Qu Z, Garfinkel A, Chen P S and Weiss J N 2000 Mechanisms of discordant alternans and induction of reentry in simulated cardiac tissue *Circulation* **102** 1664–70

[21] Riccio M L, Koller M L and Gilmour R F Jr 1999 Electrical restitution and spatiotemporal organization during ventricular fibrillation *Circ. Res.* **84** 955–63

[22] Sampson K J and Henriquez C 2001 Simulation and prediction of functional block in the presence of structural and ionic heterogeneity *Am. J. Physiol.* **281** H2597–603

[23] Waldo A L, Camm A J, deRuyter H, Friedman P L, MacNeil D J, Pauls J F, Pitt B, Pratt C M, Schwartz P J and Veltri E P 1996 Effect of d-sotalol on mortality in patients with left ventricular dysfunction after recent and remote myocardial infarction. The SWORD investigators. Survival With Oral d-Sotalol *Lancet* **348** 7–12

[24] Watanabe M A, Fenton F H, Evans S J, Hastings H M and Karma A 2001 Mechanisms for discordant alternans *J. Cardiovasc. Electrophysiol.* **12** 196–206

[25] Winfree A T 1987 *When Time Breaks Down* (Princeton, NJ: Princeton University Press)

[26] Witkowski F X, Leon L J, Penkoske P A, Giles W R, Spano M L, Ditto W L and Winfree A T 1998 Spatiotemporal evolution of ventricular fibrillation *Nature* **392** 78–82

[27] Yan G X, Shimizu W and Antzelevitch C 1998 Characteristics and distribution of M cells in arterially perfused canine left ventricular wedge preparations *Circulation* **98** 1921–7

Stimulation protocol for initiation of ventricular fibrillation; 3 methods for decreasing the risk of VF initiation

Ventricular fibrillation (VF), an extremely rapid and irregular heartbeat, is a leading cause of death in the Western world. Pharmacol gical approaches for preventing VF, which have included drugs that block sodium, calcium, and potassium channels, have been largely unsuccessful. Alternatively, implantable defibrillators can rescue a patient's heart from VF, but these devices are expensive and typically make use of a high-energy shock that can be painful and damaging to tissue. Thus, both methods for treating VF need improvement. The development and testing of both treatments require a method for assessing the ability of a treatment to prevent or halt VF. Currently, VF can be initiated in the heart by a variety of methods, but none of these methods is similar to the clinical induction of VF, which typically occurs after a few (3-10) premature ventricular activations. Recently, we developed a method for initiating VF using a computer model of normal one dimensional cardiac fibers. This model is based on the recovery properties of cardiac action potential duration and of the conduction velocity of electrical waves in the heart. The stimulus protocol consists of interrupting the normal sinus rhythm of the heart with 4 premature stimuli. If these stimuli are delivered with the appropriate timing (as predict by the model), the excitatory wave initiated by the fourth stimulus stops abruptly before reaching the end of the fiber. In two and three dimensional tissue, this "conduction block" can lead to wave break and the initiation of spiral wave reentry. Further, the model has shown that the likelihood of this conduction block occurring after the initiati n protocol is applied can be decreased by altering the recovery properties in three different ways: by altering the velocity recovery function so that conduction slows at short rest intervals, by altering the action potential duration recovery function to reduce the sensitivity of action potential duration to the preceding rest interval, and by increasing cardiac memory. Thus, this work has led to tw significant developments: 1) a stimulus protocol for initiating fibrillation in heart tissue that is similar to the clinical induction of VF and 2) three methods for altering the recovery properties of heart tissue to reduce the likelihood of VF induction.

A. Specific Aims

The studies conducted thus far for this project[1-9], coupled with the studies of several other groups[10-27], have provided substantial evidence for a key role of electrical restitution in determining the dynamical behavior of cardiac tissue. These observations may be particularly relevant for understanding (and preventing) the development of ventricular fibrillation (VF). We now plan to extend our studies to more critically evaluate the contribution of dynamically-induced heterogeneity of repolarization in the setting of intrinsic electrical heterogeneity. To achieve these goals we propose the following specific aims:

1. To determine the extent to which dynamic heterogeneity of repolarization predisposes to the development of conduction block and reentrant excitation.

Our previous studies have shown that dynamic heterogeneity of repolarization, as induced by rapid pacing, predisposes to the development of conduction block in 1-dimensional computer models and in isolated Purkinje fibers. We now propose to determine whether the delivery of 1-4 premature stimuli increases dynamic heterogeneity of repolarization and thereby precipitates conduction block. Studies will be conducted initially in computer models of a homogeneous 1-dimensional cable and in isolated Purkinje fibers, where increased spatial dispersion of repolarization during premature stimulation can be assigned principally to the development of dynamical heterogeneity.

2. To determine the extent to which dynamic heterogeneity of repolarization interacts with intrinsic heterogeneity in the development of conduction block and reentrant excitation.

Studies will be conducted in experimental preparations and computer models having intrinsic spatial gradients of repolarization. Experimental models include arterially perfused canine left ventricle and anesthetized closed-chest German shepherd dogs having an inherited predisposition to ventricular arrhythmias and sudden cardiac death.

The results of these studies will substantially improve our understanding of the mechanisms by which VF is initiated and sustained. As such, they promise to provide a basis for new and more effective therapies for the prevention of sudden cardiac death.

B. Background and Significance

Electrical restitution and spatial dispersion of repolarization

Although several theories regarding the cellular electrophysiologic mechanism for VF currently are being evaluated[17,26,28-32], substantial evidence has accumulated over the last few years to suggest that fibrillation is a state of spatiotemporal chaos consisting of the perpetual nucleation and disintegration of spiral waves[32,33], in association with a period doubling bifurcation of local electrical properties[3,12,18,34]. Nucleation of the initiating spiral wave pair is caused by local conduction block (wave break) secondary to spatial heterogeneity of refractoriness in the ventricle[32,33,35-37]. Until recently, spatial heterogeneity was thought to result solely from regional variations of intrinsic cellular electrical properties[37,38] or from stimulation at more than one spatial location[21,25,36]. However, it is now appreciated that purely dynamical heterogeneity can be sufficient to cause conduction block during single site stimulation in both homogeneous one-dimensional models of canine heart tissue and in rapidly paced canine Purkinje fibers. A similar mechanism has been shown to precipitate conduction block and spiral break up in models of homogeneous two-dimensional tissue[11].

The period doubling bifurcation implicated in the transition to conduction block is manifest as alternans, a beat-to-beat long-short alternation in the duration of the cardiac action potential [3,12,18,25,34]. Previous investigators have hypothesized that alternans can be accounted for by a simple uni-dimensional return map called the action potential duration restitution function [10,14,39,40]. This hypothesis assumes the duration of an action potential (*APD*) depends only on its preceding diastolic interval (*DI*) through some function *f(DI)* that is measured experimentally. If the APD restitution function has a slope ≥ 1, then a period doubling bifurcation occurs for some value of the pacing cycle (*BCL*), where $BCL = APD + DI$. The velocity at which an action potential propagates (*CV*) also can be described by a restitution function, where $CV = c(DI)$. More recently, other potential modulators of restitution, such as memory and calcium cycling, have been incorporated into formulations for restitution[6,11,41].

It has been shown previously that the combination of a steeply sloped APD restitution function and a monotonically increasing CV restitution function is sufficient to produce dynamical conduction block during sustained pacing at a short cycle length[1,42]. This observation may provide a generic mechanism for wave break and the onset of ventricular tachycardia and fibrillation. However, it is unlikely that the conditions used to demonstrate this phenomenon experimentally apply to the clinical situation, where the induction of ventricular tachyarrhythmias typically is associated with the interruption of normal cardiac rhythm by only a few premature beats. A single premature beat is sufficient to cause spatial heterogeneity in the form of discordant alternans[25], but the conditions required for the development of conduction block in this setting have not been studied extensively.

Therefore, we determined recently whether dynamic heterogeneity and conduction block occur in a computer model of canine heart fibers in which pacing at a slow rate is interrupted by 1-4 premature stimuli[8]. This protocol simulates the interruption of sinus rhythm by 1-4 premature ventricular complexes, a situation that can lead to the onset of ventricular fibrillation clinically. Furthermore, we determined whether the conduction block induced in this way can be accounted for by the same dynamical mechanism that underlies the development of conduction block during rapid pacing. A coupled maps model of heart tissue was used for the study, which allowed us to identify the roles that CV and APD restitution play in the development of dynamic heterogeneity. We also considered the additional contribution of cardiac memory (*M*) to the development of dynamical heterogeneity and conduction block.

As described below, these studies indicated that a short-long-short-intermediate coupling interval pattern of premature stimuli induced marked spatial dispersion of repolarization and conduction block. The dynamical mechanism for the development of block was the same as for the development of discordant alternans during sustained rapid pacing. This type of conduction block could lead to wave break and spiral wave initiation if it occurred in two- and three-dimensional tissue, provided the block was local. The development of local block would be facilitated in intact myocardium by twist anisotropy and intrinsic heterogeneity. We have elected to pursue this idea, which provides the basis for the first specific aim of this project.

An attractive experimental model for testing the hypothesis that maximizing dynamically-induced spatial heterogeneity of repolarization is conducive to the development of VF is the inherited sudden death model developed by Moïse and co-workers[43-50]. This model consists of a colony of German shepherd dogs that are afflicted with an inherited propensity for sudden death. Affected dogs have frequent ventricular arrhythmias (VA), with those exhibiting ventricular tachycardia (VT) having the highest incidence of sudden death[43]. Death is unexpected and most frequent during sleep or at rest after exercise[44]. A window of vulnerability for the presence of VA and sudden death exists between 12 and 50 weeks of age with the peak affectedness between 20 and 28 weeks of age[46]. As determined by ambulatory Holter analysis, affected dogs can have up to 50,000 ventricular premature beats and runs of rapid VT during a

24 hr recording period. Two types of VT have been identified; (1) a rapid (heart rate > 300 bpm), nonsustained, polymorphic form, and (2) a less rapid (heart rates < 250 bpm), sustained, monomorphic form[43,51,52]. The first type (85% of VT identified) is associated with sudden death and is frequently preceded by a pause. Moreover, this type of VT is most frequent during slow wave sleep, rapid eye movement (REM) sleep, and between 4 and 7 am[44]. The average incidence of sudden death in affected dogs is approximately 33%. However, the majority of affected dogs do not develop VF. The reason why most of these dogs do not develop VF, despite the presence of many episodes of rapid, polymorphic VT is unknown. In this regard, affected dogs are similar to some post-myocardial infarction patients, in that these patients may survive for years with a high incidence of VT before succumbing to sudden death[53].

The mechanism for the initiation and maintenance of VT in affected dogs has been investigated at several levels. The circumstances of death suggest that the autonomic nervous system is involved, in that the frequency of VT is greatest during rapid eye movement (REM) sleep[44]. During REM sleep[43] parasympathetic tone is high, but bursts of sympathetic tone also occur. Studies that examined sympathetic innervation to the heart using ^{123}I-metaiodobenzylguanidine scintigraphy and immunocytochemical staining for tyrosine hydroxylase revealed that large areas of the heart lack sympathetic innervation[54]. Further studies documented increased beta-receptor density, increased beta-adrenergic stimulation of adenylyl cyclase and abnormal beta-adrenergic signal transduction in the denervated regions of the heart[51,52]. In these same regions, cardiomyocytes are prone to the development of calcium oscillations, severe calcium overload, and cell death after exposure to β_1-receptor agonists[55].

In addition to abnormalities of calcium cycling, other important alterations in the ionic currents responsible for repolarization are present in these dogs[52,56,57], including a documented decrease in the density of the transient outward potassium current (I_{to}) and circumstantial evidence for decreased delayed rectifier (I_{Ks}). A reduction in outward repolarizing current presumably is responsible for the prolongation of action potential duration and development of prominent early afterdepolarizations (EADs) in left ventricular Purkinje fibers of affected dogs[50]. The EADs are the likely cause for the initiation of the pause dependent rapid polymorphic VT, the suspected initiator of VF. Abnormal T waves are seen on the surface ECG and are a reflection of the afterdepolarizations or the spatial inhomogeneity of repolarization among different regions of the left ventricle of affected dogs[49]. The latter could provide a permissive substrate for reentry arrhythmias as well.

Thus, the German shepherd model provides an opportunity to determine whether certain patterns of multiple premature beats (secondary to EAD-induced triggered activity) are sufficient to induce VF in the setting of significant intrinsic heterogeneity of repolarization (secondary to repolarization alterations associated with sympathetic denervation). As discussed below under Preliminary Studies, we have begun to investigate whether patterns of premature stimuli designed to maximize spatial dispersion of repolarization via augmentation of dynamic heterogeneity initiate VF in these animals. Moreover, we also are testing whether the spontaneously occurring VT cycle lengths in these animals typically do not induce VF because they do not augment dynamically-induced spatial dispersion of repolarization sufficiently.

C. Preliminary Studies

Dynamically-induced spatial dispersion of repolarization

Our previous theoretical and experimental studies of the impact of dynamic heterogeneity of repolarization on the development of conduction block were conducted in computer models of a homogenous 1-dimensional cable and in isolated Purkinje fibers during fixed pacing. As the pacing cycle length was shortened progressively, a transition from 1:1 phase locking to a concordant alternans (2:2 locking) to discordant alternans to intermittent 2:1 conduction block

occurred[1]. These results confirmed the predictions of previous computer modeling studies of these phenomena[25] and extended experimental observations that the development of discordant alternans was associated with local conduction block and the initiation of reentry[19,59]. In addition, they demonstrated that complex dynamics was possible in a homogenous 1-dimensional cable, in the absence of intrinsic heterogeneity or anisotropy, and that the mechanism for the dynamics could be described using simple unidimensional maps for the restitution of APD and CV.

The evolution of dynamics during fixed pacing occurs relatively gradually, which allows this phenomenon to be studied in the quasi-steady-state. As a result, a detailed description of the dynamics and identification of the underlying mechanism is possible. It is unlikely, however, that prolonged activation at a short constant cycle length initiates VF in patients at risk for sudden death. Therefore, we recently have begun to investigate a scenario that is more common in such patients – initiation of VF following a run of non-sustained VT. For these studies, computer models of a homogenous 1-dimensional cable were generated using a coupled maps memory model[6] and an ionic model[2]. The models were paced at a cycle length of 1000 or 500 ms for 50 beats, after which a series of premature stimuli was delivered (Figures 1 and 2). Premature stimuli delivered at short DI (e.g., S_2 in Figure 2) elicited action potentials at the site of stimulation that, in accordance with the relevant APD and CV restitution relations,

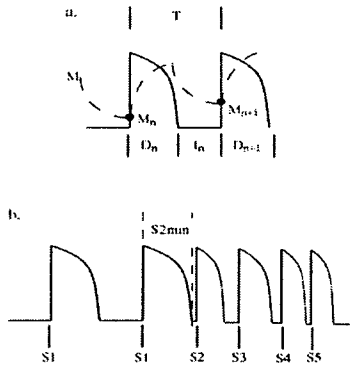

Figure 1. Schematic drawings of: *a.* the coupled maps memory model, where action potential duration (D) is a function of the diastolic interval (I) and memory (M) during pacing at a fixed interval (T) and; *b.* the stimulation protocol to maximize spatial dispersion of repolarization.

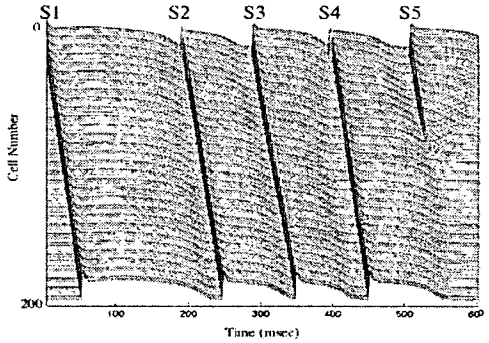

Figure 2. Spatial dispersion of repolarization induced in an ionic model of a homogenous 1-dimensional cable by multiple premature stimuli (as in figure 3b). Note that short duration action potentials at the site of stimulation increase in duration as they propagate along the fiber, whereas long duration action potentials shorten. The resulting discordant alternans pattern culminates in conduction block.

were short in duration and conducted slowly. Slow conduction along the fiber provided progressively more recovery time as the action potential conducted down the fiber. Accordingly, DI increased along the fiber, as did the corresponding APD, resulting in a discordance between APD at the site of stimulation and at the distal end of the fiber. Conversely, premature stimuli delivered at longer DI (S_3 in Figure 2) produced longer duration action potentials that conducted more rapidly. The more rapidly conducting action potentials impinged progressively on the preceding DI as they conducted along the fiber, creating a shorter DI and corresponding APD. Once again, discordant APD between the site of stimulation and the distal end of the fiber resulted. The spatial dispersion of repolarization caused by this sequence of cycle lengths could be amplified by the delivery of multiple premature stimuli, eventually resulting in conduction block (S_5 in Figure 2).

To more completely characterize this sequence of events, we determined all possible combinations of S_2-S_5 that produced conduction block in the coupled maps model (block also occurred with many fewer combinations of S_2-S_3 and many more combinations of S_2-S_7). Although approximately 67,000 combinations produced conduction block, the distribution of such combinations was not random, but was clustered according to specific S_2 and S_3 intervals, as shown in Figure 3. The incidence of block was greatest when S_2 was delivered at a coupling interval near S_1S_{2min} (the shortest S_1S_2 interval that produced a propagated response) and S_3 was delivered at a coupling interval approximately 50 ms longer than S_2S_{3min}. Although not shown on this 3-dimensional plot, the S_3S_4 interval most often associated with block was near S_3S_{4min}, whereas the S_4S_5 interval was approximately 10 ms longer than S_4S_{5min}. This short-long-short-intermediate pattern of stimulation produced discordant alternans and conduction block of the type shown in Figure 2. In this study we also determined the impact of changes in the slope of the APD restitution relation, the magnitude of memory, the shape of the CV restitution relation and the strength of cell coupling. In general, the incidence of conduction block was reduced by decreasing the slope of the APD restitution relation, increasing memory, increasing cell coupling and extending the CV restitution relation to permit slow conduction (thereby preventing "head-tail" interactions)[8].

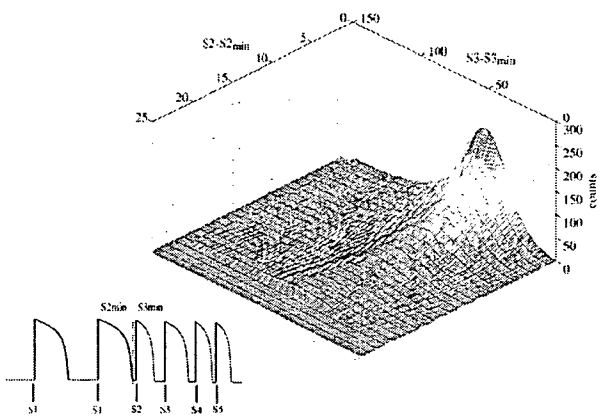

Figure 3. Incidence of conduction block (counts – right axis) following the delivery of 4 premature stimuli (see protocol, lower left) in the coupled maps memory model. Results are shown for combinations of the S_1S_2 and S_2S_3 intervals, referenced to S_{2min} and S_{3min}, respectively (S_4 and S_5 not shown).

More recently, we have begun to investigate whether dynamically-induced spatial dispersion of repolarization promotes the development of conduction block and reentrant excitation in settings where underlying intrinsic heterogeneity is present. To that end, the sequence of premature stimulus intervals predicted by the computer model to cause conduction block was delivered to the right ventricles of closed chest anesthetized normal beagles and MAP recordings were obtained from the right and left ventricles. The dogs initially were paced at a cycle length of 400 ms and a single premature stimulus (S_2) was delivered at progressively shorter S_1S_2 intervals until S_2 failed to capture (S_1S_{2min}). The S_1S_2 interval was then set to S_1S_{2min} + 40 ms and an S_3 stimulus was delivered at progressively shorter S_2S_3 intervals until $S_{3min}$was encountered. The procedure was then repeated to find S_{4min} and S_{5min}. Thereafter, a sequence of premature stimuli consisting of S_1S_{2min} + 5 ms, S_2S_{3min} + 50 ms, S_3S_{4min} + 5 ms and S_4S_{5min} + 5-10 ms was delivered. As shown in Figure 4, the patterns of APD produced by this sequence of premature cycle lengths (CL_{VF}) was similar to that produced in the computer models (c.f. Figure 2). Short duration responses (S) at the RV recording site were associated with longer duration responses (L) at the LV site and vice versa and the pattern of discordant alternans preceded the development of VF.

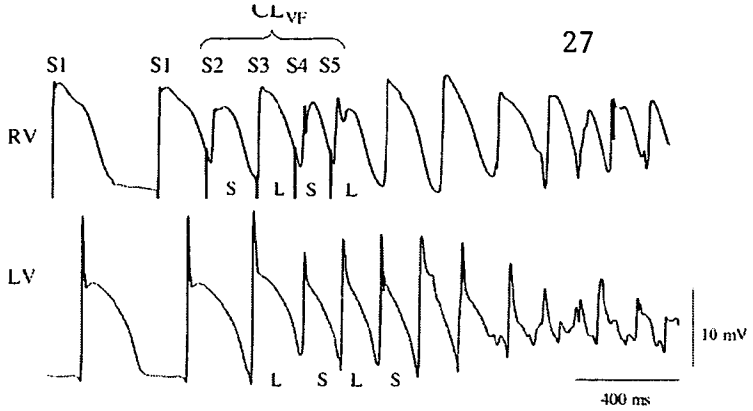

Figure 4. Examples of MAP recordings obtained from the right (RV) and left (LV) ventricles of a closed-chest anesthetized beagle during delivery of multiple premature stimuli (CL_{VF}) to the RV. CL_{VF} were chosen to produce maximum dynamically-induced dispersion of repolarization, as predicted from the results of the coupled maps model shown in Figure 3.

The delivery of CL_{VF} has produced VF in all 8 dogs tested thus far, whereas the delivery of multiple premature stimuli at sequentially shorter cycle lengths has failed to induce VF in any of the dogs (Figure 5). Although we have not, for obvious reasons, tested all 67,000 possible combinations of cycle lengths predicted to cause conduction block in the model, nor have we tested more than a few of the intervals that are not expected to cause block, the highly reproducible induction of VF by CL_{VF} lying near the peak of the plot shown in Figure 3 suggests that stimulus protocols designed to maximize dynamically-induced spatial heterogeneity of repolarization may reliably promote the induction of VF. The exact nature of the spatial dispersion produced by such a protocol will require more extensive mapping than can be accomplished by two MAP recordings, but the observation that CL_{VF} produces discordant alternans between at least 2 RV and LV recording sites suggests that the pattern of APD generated by the computer models may pertain to the intact heart.

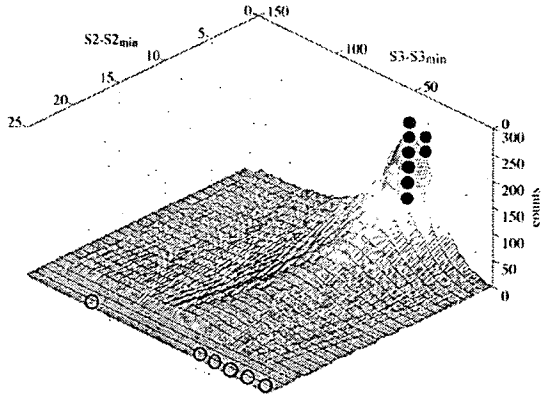

Figure 5. Incidence of conduction block following the delivery of 4 premature stimuli in the coupled maps memory model (Figure 3), and following the delivery of CL_{VF} in anesthetized beagles (filled circles). CL_{VF} induced VF in all 8 dogs. In contrast, patterns of cycle lengths that fell outside CL_{VF} did not induce VF (unfilled circles).

As a further test of the hypothesis that dynamically-induced spatial heterogeneity is arrhythmogenic, we determined whether a reduction in the slope of the APD restitution relation suppresses the development of spatial heterogeneity APD and conduction block during premature stimulation, as shown in the computer model[8]. For these studies, we tested the effects of verapamil, which is known to decrease the slope of the dynamic restitution relation [5], in the anesthetized closed chest dogs described above (n = 8). MAP duration (MAPD) was measured in RV and LV endocardium during programmed stimulation of the RV using 4 appropriately timed premature stimuli (S_2-S_5), following a train of 20 stimuli at a constant S_1S_1 interval of 400 ms. The stimulation protocol incorporated the same short-long-short-intermediate sequence shown in Figure 5, adjusted as necessary to account for changes in S_{2min}-S_{5min} produced by verapamil. VF induction was attempted during control and 30 minutes after i.v. verapamil (0.1, 0.3 or 1.0 mg/kg/min).

VF induction occurred in all dogs during control and after 0.1 mg/kg verapamil and was associated with discordant alternans of MAPD between RV and LV. In contrast, after the two higher verapamil doses MAPD alternans was reduced in magnitude and was concordant and VF could not be induced. These effects were not associated with significant changes in the slope of the standard (S_1S_2) MAPD restitution relation, which was 0.41 $\pm$ 0.17 during control and was 0.47 $\pm$ 0.28, 0.56 $\pm$ 0.20 and 0.39 $\pm$ 0.18 after verapamil. Thus, suppression of spatial APD heterogeneity by verapamil was associated with an inability to induce VF using premature

stimuli. However, the doses of verapamil required to produce this effect had significant negative dromotropic, chronotropic and inotropic effects: verapamil increased the PR interval (from 84.7 ± 3.8 during control to 111.8 ± 12.2, 132.0 ± 15.0 and 139.5 ± 18.0 ms after verapamil), decreased heart rate (from 139.0 ± 9.7 to 110.0 ± 2.1, 101.6 ± 3.8, and 95.2 ± 8.8 bpm) and decreased mean blood pressure (from 116.8 ± 7.3 to 107.4 ± 11.4, 108.0 ± 6.3 and 101.2 ± 9.4 mmHg). These results suggest that suppression of VT-induced spatial electrical heterogeneity may be one means of preventing VF, but that verapamil is unlikely to be the drug of choice for producing such an effect in patients.

Although the induction of VF by CL_{VF} in normal beagles confirms the predictions made by the computer models, this result is somewhat expected, in that the data used to construct the models was obtained from normal canine myocardium. This model has the additional limitation of requiring external stimuli to induce VF, since these dogs do not have spontaneous ectopy. To test the predictions from the computer model more rigorously, we next investigated whether CL_{VF} induced VF in German shepherd dogs that display non-sustained polymorphic VT and have an inherited predisposition to sudden death (Figure 6). As discussed above, one of the interesting and unanswered questions with respect to these animals is why they often live for months with multiple episodes of rapid, polymorphic VT before succumbing to sudden death. Based on the response of the beagles to CL_{VF}, it seems possible that the German shepherds, despite having copious amounts of ectopy, do not die sooner because they do not routinely generate the proper sequence of coupling intervals, insofar as promoting dynamically-induced spatial dispersion of repolarization is concerned.

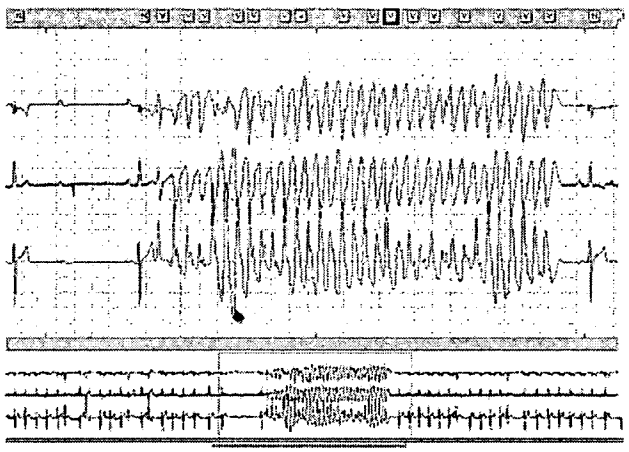

Figure 6. Spontaneous non-sustained polymorphic ventricular tachycardia in a German shepherd dog.

As an initial test of this idea, 5 affected German shepherd dogs were anesthetized and instrumented as described above for the beagles. CL_{VF} were determined from measurements of S_{2min}-S_{5min} and predictions from the beagle–based computer model and were delivered to the RV or LV. VF was induced in 3 of the dogs, but not in the other two, even after several adjustments of the CL_{VF}. Sequences of cycle lengths obtained from Holter recordings during multiple episodes of polymorphic VT (CL_{VT}) also were delivered to the dogs. None of these sequences induced VF. The sequences during CL_{VT} consisted of progressively shorter cycle lengths, in contrast to CL_{VF}, which were short-long-short-short. In addition, even during longer runs of non-sustained VT, such as the run shown in Figure 6, a CL_{VF} – type pattern did not occur. This observation raises the question of why do the German shepherds eventually die suddenly? Unfortunately, despite the hundreds of Holter recordings obtained since this colony was established, VF has never been captured. To remedy this situation, we currently are implanting Reveal Plus© (Medtronic) event recorders in severely affected dogs. Thus far, we have captured the development of VF in one dog. The sequence of cycle lengths preceding VF was similar to that used to precipitate VF in the programmed stimulation studies, but clearly more episodes of spontaneous VF need to be captured and analyzed before definitive conclusions can be drawn.

D. Research Design and Methods

Specific Aim #1.

Experimental plan

The mechanism for conduction block following the delivery of multiple premature stimuli will be studied initially using a one-dimensional computer model of a canine heart fiber, as described previously[1]. The fiber will be stimulated at one end at a cycle length near normal canine sinus rhythm (S_1S_1=500 ms). After 10 S_1 stimuli, 4 premature stimuli (S_2, S_3, S_4 and S_5) will be delivered. The coupling intervals of the premature stimuli will be varied and conduction of the resultant responses observed. For each combination of premature stimuli, one of three outcomes is possible: 1) the stimulus elicits an action potential that propagates along the entire fiber; 2) the stimulus does not elicit a propagated response (Type I block); 3) the stimulus elicits an action potential that blocks before reaching the end of the fiber (Type II block).

To assess the vulnerability of the simulated tissue to Type II block, the $S_2S_3S_4S_5$ combinations will be applied as follows: the S_1S_2 interval will be varied from the minimum value that conducts (S_1S_{2min}) to S_1S_{2min} + 20 ms. For each S_1S_2 interval, the S_2S_3 interval and the S_3S_4 interval will be varied in combination from the minimum value that conducts up to a value of 250 ms for each interval. For each $S_2S_3S_4$ combination that conducts, the S_4S_5 interval will be varied from the minimum interval that generates an action potential at the site of stimulation to the minimum interval that generates an action potential that conducts down the entire fiber. If no $S_2S_3S_4S_5$ combination is found that produces conduction block for more than a 20 ms window in either the S_2S_3 interval or the S_3S_4 interval, the search is halted for that interval. Intervals are varied in steps of 1ms.

The computer model currently is based on the coupled maps memory model, which may not replicate certain aspects of the dynamics during premature stimulation[41]. Accordingly, future versions of the model will incorporate the results obtained from the standard restitution protocol for each of the four premature stimuli. The results generated by the latter model will be compared with the results generated by the current model and will be evaluated with respect to the success or failure of the CL_{VF} predicted by the different models to induce VF in the arterially perfused left ventricular preparations and in the whole animal experiments (see below). Other models of restitution[11,41] also may be tested, as warranted. The restitution relations for APD and CV in the current model were derived from data obtained from canine endocardium. In future versions of the model, these functions will be obtained from epicardial and mid-myocardial layers of myocardium as well.

Once the effects of multiple premature stimuli on spatial dispersion of repolarization have been determined in the homogenous computer model, simulations will be conducted in the coupled maps model after introduction of a spatial gradient of intrinsic repolarization, using a modified version of the method of Henry and Rappel[60]. The repolarization gradient and pattern of cell coupling will be designed to mimic the transmural gradient of repolarization reported for canine myocardium[61-63]. The interactions between intrinsic and dynamic heterogeneity of repolarization also will be studied in 2- and 3- dimensional computer models, as they become available as the result of studies to be conducted in collaboration with Drs. Jeffrey Fox and Wouter-Jan Rappel ("Computer model of the canine ventricle", supported by HL075515).

Once the results of the computer simulations are known, experiments will be conducted in isolated canine Purkinje fibers. These experiments should, based on our previous experience[1], be an appropriate test of the effects of multiple premature stimuli on spatial dispersion of repolarization in a (nearly) homogenous, (functionally) 1-dimensional cable. Thereafter, the effects of CL_{VF} will be tested in isolated arterially perfused canine left ventricle, a preparation capable of generating VF[5]. Tests of the CL_{VF} protocol also will be conducted in normal beagle dogs, where the results generated by the computer model, which is based on data obtained

from such hearts, is expected to be relevant (Figures 4 and 5). Finally, the CL_{VF} protocol will be tested in German shepherd dogs having an inherited predisposition to sudden death.

The details of the various experimental protocols are given in the following sections.

One-dimensional computer models

Our initial studies will be conducted using a coupled maps model of a one-dimensional cardiac fiber, as described previously[1,94]. The model is based on the equation

$$I_{n+1}(x_i) = T_{n+1}(x_i) - D_{n+1}(x_i). \quad (1)$$

$T_{n+1}(x_i)$ is the time interval between activations of site x_i. It is determined by including the time delays caused by the propagation from the pacing site to site x_i, which yields

$$T_{n+1}(x_i) = \tau + \sum_{j=0}^{i-1} \frac{\Delta x}{V_{n+1}(x_j)} - \sum_{j=0}^{i-1} \frac{\Delta x}{V_n(x_j)} \quad . \quad (2)$$

τ is the time interval between activations applied to the pacing site and $\Delta x=0.1$ is the length of a single cell (time units in ms and space units in mm). The conduction velocity $V_n(x_i)$ depends only on I through the velocity recovery function $V_n = c(I_n)$ given by $c(I)=V_{max}(1-exp(-(I+\beta)/\delta))$. $V_{max}=0.72$, $\delta=14$, and β is varied to adjust the value of V at $I=I_{min}$. D is determined locally based on a memory model mapping[94] given by:

$$\begin{aligned} M_{n+1} &= g(M_n, I_n, D_n) = e^{-I_n/\tau_m}\left[1 + (M_n - 1)e^{-D_n/\tau_m}\right] \\ D_{n+1} &= f(M_{n+1}, I_n) = (1 - \alpha M_{n+1})\left(A + \frac{B}{1 + e^{-(I_n - C)/\tau_D}}\right). \end{aligned} \quad (3)$$

τ_m is the time constant for memory. $A = 88$, $B = 122$, $C = 40$, and $\tau_m = 180$[94]. α determines the influence of memory on D, and τ_D is used to adjust the dependence of the D recovery function on I. Coupling between sites is included by using the diffusion terms from Echebarria and Karma[95]. Including diffusion then yields

$$D_{n+1} = f(M_{n+1}, I_n) + \xi^2 \nabla^2 D_{n+1} - w \nabla D_{n+1}, \quad (4)$$

with $\xi = 1.0$ and $w = .35$. Discretizing the derivatives produces a tri-diagonal linear system of equations that can then be solved easily. The defining equation for the model is therefore

$$\begin{aligned} M_{n+1} &= g(M_n, I_n, D_n) \\ D_{n+1} &= f(M_{n+1}, I_n) + \xi^2 \nabla^2 D_{n+1} - w \nabla D_{n+1} \\ I_{n+1}(x_i) &= \tau + \sum_{j=0}^{i-1} \frac{\Delta x}{c(I_{n+1}(x_j))} - \sum_{j=0}^{i-1} \frac{\Delta x}{c(I_n(x_j))} - D_{n+1}(x_i) \end{aligned} \quad (5)$$

Cellular action potentials and wave propagation will be simulated using a modified version the Winslow ionic model,[66] as described in detail[2,67]. Briefly, compared to the native Winslow model, I_{K1} is decreased at depolarized potentials.[56] The maximum conductance and rectification of I_{Kr} are increased and activation kinetics are slowed. I_{Ks} is increased in

magnitude and activation shifted to less positive voltages.[68] L-type calcium current is modified to produce a smaller, rapidly inactivating current. Finally, a simplified form of intracellular calcium dynamics is used[69]. The PDE for a one-dimensional piece of tissue will be solved numerically, as described by Qu *et al.*[20] The length of the one-dimensional cable is set to 220 cells (30 cells longer than the minimum length required for the development of at least one node), with the length of each cell = 200 μM, and a diffusion coefficient of .001 cm^2/msec.

Isolated Purkinje fibers

Adult beagle or mongrel dogs weighing 10-30 kg will be anesthetized with Fatal-Plus (86 mg/kg i.v.) and their hearts will be excised rapidly[5]. Free running Purkinje fibers 1.5-2.5 cm in length and 1-2 mm in width are excised from either ventricle, mounted in a Plexiglas chamber and superfused with Tyrode solution at 15 ml/min. The Tyrode solution is bubbled with 95% O_2 and 5% CO_2. The PO_2 is 400-600 mmHg, the pH is 7.35 ± 0.05 and the temperature is 37.0 ± 0.5 °C. The composition of the Tyrode (in mM) is: $MgCl_2$ 0.5, NaH_2PO_4 0.9, $CaCl_2$ 2.0, NaCl 137.0, $NaHCO_3$ 24.0, KCl 4.0 and glucose 5.5. The fibers are stimulated using rectangular pulses of 2 ms duration and 2-3 times the diastolic threshold (0.1-0.3 mA), delivered through Teflon-coated bipolar silver electrodes. Transmembrane action potentials recordings are obtained simultaneously from 4-6 sites along the fiber. The recordings are sampled at 2 kHz with 12-bit resolution using custom data acquisition programs written in Linux and run on a PC.

The dependence of APD on the preceding DI will be determined using a standard restitution protocol and a dynamic protocol, as described previously[9]. For the standard protocol, single test pulses (S_2) are delivered after every 20th basic pulse (S_1) at BCL = 400 ms. The S_1S_2 coupling interval is progressively shortened in steps of 10-20 ms starting from 300 ms until the premature stimulus fails to capture. The duration of the action potential elicited by S_2 is measured at 95% of repolarization (APD_{95}) and is plotted as a function of the preceding DI, where the DI equals the S_1S_2 interval minus APD_{95} of the response to the last S_1 stimulus. This procedure will be repeated to measure restitution following delivery of an S_3, S_4 and S_5 stimulus, to generate data comparable to those generated in the whole dog experiments.

The relationship between APD and DI also will be determined during pacing at a constant BCL (dynamic restitution). The BCL is shortened from 400 to 200 ms in steps of 50 ms and from 200 ms to the effective refractory period in steps of 5-10 ms. At BCL that produce a 1:1 stimulus:response locking, pacing is stopped after steady state has been reached and APD_{95} of the last paced action potential is measured. During APD alternans, pacing is interrupted twice to directly measure APD_{95} of both the long and the short action potential.

The restitution data will be entered into the coupled maps computer model to generate sequences of multiple premature stimuli that maximize dynamically-induced spatial dispersion of repolarization and precipitate conduction block. The model-generated cycle lengths will then be delivered to the Purkinje fiber and the spatial patterns of APD and the incidence of conduction block determined. Cycle length sequences generated from both the standard and dynamic restitution relations will be tested to determine which sequence produces spatial patterns in the fiber that most closely agree with those predicted by the model. If the spatial patterns produced by both of these sequences differs significantly from that predicted by the model, the coupled maps model will be modified by altering the configuration for memory.

Specific aim # 2

Arterially perfused left ventricle

Adult beagle or mongrel dogs or juvenile affected German shepherd dogs will be anesthetized as described above and their hearts will be excised rapidly and placed in cool Tyrode solution[5]. The circumflex coronary artery or a branch of the right coronary artery will be

cannulated using PE tubing and a transmural section of tissue measuring 30-50 mm in width, 30-90 mm in length and 10-18 mm in depth excised. The preparation is suspended in a Plexiglas chamber with the epicardial or endocardial surface facing up or is placed on-end, to allow recordings to be obtained from both surfaces simultaneously. The preparation is perfused via the coronary artery and is superfused with normal Tyrode solution at a flow rate of 35 ml/min. Perfusion pressure is 50-80 mm Hg and the temperature is 37.0 - 38.0°C.

Electrical activity will be mapped using arrays of 64 monophasic action potential (MAP)-type recording electrodes, supplemented by 1-4 floating glass microelectrodes. In those experiments for which transmural recordings are required, 2-3 roving MAP electrodes or floating microelectrodes will be lowered onto the uppermost transmural edge of the preparation. The MAP and transmembrane action potential recordings are displayed on a storage oscilloscope and a computer monitor and are sampled at 1250 Hz with 12-bit resolution. The MAP signals are high-pass (cutoff = 0.15 Hz) and low-pass filtered (cutoff = 600 Hz). Records of 4-7 seconds duration are obtained every 20-40 seconds during the course of the experiment.

The standard and dynamic restitution relations will be determined from microelectrode or MAP recordings obtained from epicardium, endocardium and midmyocardium, with the latter being accessed from the exposed transmural edge of the preparation. For epicardial and endocardial measurements, action potentials will be recorded from several sites from base to apex, with the expectation that a gradient of APD and restitution kinetics will exist. Following measurement of the restitution relations, multiple premature stimuli will be delivered to the preparations and their effect on spatial dispersion of repolarization, the development of conduction block and the induction of VF will be determined.

Intact beagle dogs

We plan to complete our studies using normal beagle dogs and have provided for such studies in our application for a Scientist Development Grant from the National American Heart Association. However, because the term of this application is 3 years, compared with a term of 4 years for the national award, we have elected to not include the studies of beagle dogs in this application, so that Dr. Gelzer may move forward sooner with the other studies. If this award is funded, the beagle studies will be competed by a cardiology resident, with assistance and financial support from Drs. Moïse and Gilmour, using other resources.

Intact German shepherd dogs

Studies will be conducted in German shepherd dogs having frequent ventricular premature complexes and non-sustained ventricular tachycardia (VT). Surface ECG recordings will be acquired using 24 hr ambulatory Holter monitoring. All data will be stored on 350 MB removable PC flashcards and automated Holter analysis will be performed using the Vision Premier™ software (Spacelabs Burdick Inc.). In each dog a set of 25 coupling intervals of spontaneous runs of VT (first 5 successive RR intervals of several episodes) will be measured to generate a library of coupling intervals (CL_{VT}) to be used for programmed stimulation. On the day of the study, the dogs will be induced using pentobarbital (20 mg/kg IV) and maintained with a continuous rate infusion of pentobarbital (5 mg/kg/hr) and fentanyl dihydrogen citrate (0.004 mg/kg/hr). Introducer sheets will be placed percutanously into the right femoral vein and artery and MAP recording catheters will be advanced into the RV and LV apex. These catheters are used both for cardiac pacing and for MAP recording. The MAPs and a standard surface ECG will be recorded using a multi-channel physiologic recorder (Biopac Systems, Inc).

The APD restitution relation will be determined using a dynamic restitution protocol, as described previously[9]. Briefly, the RV or LV will be paced at S_1S_1 = 400 ms for 50 beats and then at progressively shorter S_1S_1 intervals. The APD restitution relation will be determined by

plotting APD at 90% of repolarization (APD_{90}) of the last paced beat at each BCL as a function of the preceding DI. APD restitution also will be determined using a standard protocol, where the RV or LV will be paced at S_1S_1 = 400 ms for 20 beats and then at progressively shorter S_1S_2 intervals, until the S_2 stimulus fails to generate a propagated response. The S_1S_2 interval will then be set to 40 ms longer than the longest S_1S_2 interval that failed to capture and an S_3 stimulus will be delivered at progressively shorter S_2S_3 intervals, until the S_3 stimulus fails to capture. This procedure will then be repeated using an S_4 and an S_5 stimulus.

Once the APD restitution relations have been determined, the RV or LV will be paced at S_1S_1 = 400 ms for 20 beats, followed by a specific set (CL_{VT}) of premature stimuli ($S_2S_3S_4S_5$) obtained from the library of coupling intervals that occurred during spontaneous VT. The RV or LV will then be paced at S_1S_1 = 400 ms for 20 beats, followed by a specific set (CL_{VF}) of premature stimuli ($S_2S_3S_4S_5$) that are expected, based on calculations using the computer model, to produce conduction block and VF. If VF occurs, the dogs will be converted to sinus rhythm using external cardioversion/defibrillation.

Limitations

A potential limitation of the studies proposed for this project is that the spatial complexity of repolarization in the intact heart will not be recreated in the computer models. However, previous studies in which a simple computer model has been used to predict the behavior of actual myocardium have been remarkably successful not only in predicting, but also in providing a mechanistic explanation for, complex dynamical behavior related to the initiation and perpetuation of ventricular tachyarrhythmias[1]. Consequently, the studies outlined in this proposal are likely to provide important, robust mechanistic insights that can be refined as necessary at a latter date when more realisitc computer models of the heart become available.

A related limitation applies to the proposed studies of isolated cardiac tissue and intact hearts. In these studies, the complexity of actual cardiac tissue will be present, but the mapping techniques to be used will not be capable of fully evaluating that complexity. To do so would require simultaneous measurements of electrical activty from all sites, or at least from representative sites, throughout the heart. Nevertheless, even though the full range of spatial dynamics may not be captured in these studies, the proposed experiments are highly likely to indicate whether dynamically-induced heterogeneity of repolarization is an important determinant for the induction of VF. In the future, we anticipate that we will have the capability of recording electrical activity transmurally using nanofabricated multielectrode arrays. These devices currently are under development and support for this project has been requested. (NIH R01 HL073644-01, "MEMs sensors for arrhythmia detection and intervention", R.F. Gilmour Jr., PI, E. Bodenschatz, A. Lal, B. Lerman and D. C. Christini, Co-Investigators).

Although we will evaluate the predictions from the computer models regarding which combinations of premature stimuli are likely to induce VF using isolated myocardium and intact hearts, it seems likely that the electrophysiological substrates in those preparations may differ significantly from those present in patients with ischemic heart disease or various cardiomyopathies. Consequently, the proposed studies will need to be extended in the future to experimental circumstances that mimic the substrates in patients at risk for sudden cardiac death. In that regard, we envision future studies in acutely ischemic myocardium, similar to those we have conducted previously, and in a pacing-induced heart failure model, where recent studies have indicated that augmented intrinsic dispersion of repolarization provides a permissive substrate for the development of reentrant arrhythmias[108].

A final limitation (or caution) relates to the overall hypothesis that steep restitution of APD predisposes to dynamically-induced dispersion of repolarization following premature stimulation and that the latter can be used to establish the risk for development of VF.

Programmed stimulation to identify patients at risk for sudden death and to evaluate the efficacy of therapy to prevent sudden death has, of course, been tried, with very disappointing outcomes[109]. Consequently, the results of the proposed studies need to be interpreted in light of the realization that cellular electrical dynamics is unlikely to be predicted with absolute fidelity by simple models and that provocative tests that yield useful information in one setting may not necessarily be useful in a different setting. In that regard, the mode of programmed stimulation used in CAST and other such studies was designed primarily to probe intrinsic heterogeneity of refractoriness. The studies outlined in this proposal are designed to provoke and to evaluate dynamical heterogeneity, alone or superimposed on intrinsic heterogenity. It seems likely that although our preliminary experiments in the normal beagles indicate that patterns of stimulation based solely on dynamical heterogenity reliably induce VF, intrinsic heterogeneity may need to be considered more fully in order for useful predictions to be generated for diseased myocardium.

Ethical aspects of the proposed research

Adult beagles or German shepherd dogs will be anesthetized with Fatal-Plus (390 mg/ml pentobarbital sodium; Vortech Pharmaceuticals; 86 mg/kg IV). Hearts will be removed via a thoracotomy and segments of the heart placed in a tissue bath for further study. All experiments have been approved by the Institutional Animal Care and Use Committee of the Center for Research Animal Resources at Cornell University. The animals will be housed at the AAALAC accredited Laboratory Animal Services facility at the College of Veterinary Medicine, Cornell University. Excellent support service and veterinary care are provided.

The use of animal tissue is necessary because there is no currently available mathematical or computer model that adequately simulates the complex three-dimensional environment associated with the initiation and perpetuation of the type of heart rhythm disorders we plan to study. Canine hearts are used because their cardiac electrophysiological properties are similar to those of many other species, including humans, and their hearts are large enough to permit initiation and recording of rhythm disturbances. In addition, canine hearts have been studied extensively by other investigators, which facilitates data comparisons.

WHAT IS CLAIMED:

1. A method of evaluating the effect of a physiological condition on the occurrence of ventricular fibrillation, said method comprising:

providing a test system;

initiating a ventricular fibrillation inducing sequence in the test system by interrupting normal sinus heart rhythm with premature electrical stimuli;

initiating a ventricular fibrillation recovery sequence in the test system following said initiating a ventricular fibrillation inducing sequence;

subjecting the test system to a physiological condition to be tested before, during, or after said initiating a ventricular fibrillation recovery sequence; and

identifying physiological conditions which affect ventricular fibrillation recovery in the test system.

2. The method according to claim 1, wherein the said physiological condition to be tested is velocity restitution.

3. The method according to claim 1, wherein the said physiological condition to be tested is action potential duration restitution.

4. The method according to claim 1, wherein the said physiological condition to be tested is cardiac memory.

5. The method according to claim 1, wherein said initiating a ventricular fibrillation inducing sequence is carried out by initiating 4 premature stimuli under conditions effective to initiate an excitatory wave.

6. The method according to claim 1, wherein said initiating a ventricular fibrillation recovery sequence is carried out by altering velocity recovery function to slow conduction at shorter rest intervals.

7. The method according to claim 1, wherein said initiating a ventricular fibrillation recovery sequence is carried out by altering action potential duration recovery function to reduce sensitivity of action potential duration to a preceding rest interval.

8. The method according to claim 1, wherein said initiating a ventricular fibrillation recovery sequence is carried out by increasing cardiac memory.

9. The method according to claim 1, wherein the test system is selected from the group consisting of a test animal, a tissue, a cell culture, or an *in vitro* system.

10. The method according to claim 9, wherein the test system is a test animal.

11. A method of identifying treatment candidates as therapeutic strategies for prevention of ventricular fibrillation, said method comprising:

providing a test system;

initiating a ventricular fibrillation inducing sequence in the test system by interrupting normal sinus heart rhythm with premature electrical stimuli before, during, or after administering the treatment candidate to the test system; and

identifying treatment candidates which prevent said initiating from inducing ventricular fibrillation as therapeutic strategies for prevention of ventricular fibrillation.

12. The method according to claim 11, wherein the treatment candidate is a pharmaceutical compound.

13. The method according to claim 12, wherein the pharmaceutical compound is a calcium channel antagonist.

14. The method according to claim 11, wherein the treatment candidate is one or more electrical impulses.

15. The method according to claim 11, wherein said identifying identifies treatment candidates which achieve velocity restitution values consistent with histograms b and c of Figure 4 in "Dynamic Mechanism for Conduction Block in Heart Tissue" as therapeutic strategies for prevention of ventricular fibrillation.

16. The method according to claim 11, wherein said identifying identifies treatment candidates which achieve potential duration restitution values consistent with histograms b and c of Figure 5 in "Dynamic Mechanism for Conduction Block in Heart Tissue" as therapeutic strategies for prevention of ventricular fibrillation.

17. The method according to claim 11, said identifying identifies treatment candidates which achieve cardiac memory values consistent with histograms b and c of Figure 6 in "Dynamic Mechanism for Conduction Block in Heart Tissue" as therapeutic strategies for prevention of ventricular fibrillation.

18. The method according to claim 11, wherein the test system is selected from the group consisting of a test animal, a tissue, a cell culture, or an *in vitro* system.

19. The method according to claim 18, wherein the test system is a test animal.

20. The method according to claim 11, wherein said initiating a ventricular fibrillation inducing sequence is carried out by initiating 4 premature stimuli under conditions effective to initiate an excitatory wave.

21. A method of identifying treatment candidates as therapeutic strategies for treating ventricular fibrillation, said method comprising:

providing a test system;

initiating a ventricular fibrillation inducing sequence in the test system by interrupting normal sinus heart rhythm with premature electrical stimuli resulting in ventricular fibrillation in the test system;

administering the treatment candidate to the test system undergoing ventricular fibrillation; and

identifying treatment candidates which modulate ventricular fibrillation as therapeutic strategies for treatment of ventricular fibrillation.

22. The method according to claim 21, wherein the treatment candidate is a pharmaceutical compound.

23. The method according to claim 22, wherein the pharmaceutical compound is a calcium channel antagonist.

24. The method according to claim 21, wherein the treatment candidate is one or more electrical impulses.

25. The method according to claim 21, wherein said identifying identifies treatment candidates which achieve velocity restitution values consistent with histograms b and c of Figure 4 in "Dynamic Mechanism for Conduction Block in Heart Tissue" as therapeutic strategies for prevention of ventricular fibrillation.

26. The method according to claim 21, wherein said identifying identifies treatment candidates which achieve potential duration restitution values consistent with histograms b and c of Figure 5 in "Dynamic Mechanism for Conduction Block in Heart Tissue" as therapeutic strategies for prevention of ventricular fibrillation.

27. The method according to claim 21, said identifying identifies treatment candidates which achieve cardiac memory values consistent with histograms b and c of Figure 6 in "Dynamic Mechanism for Conduction Block in Heart Tissue" as therapeutic strategies for prevention of ventricular fibrillation.

28. The method according to claim 21, wherein the test system is selected from the group consisting of a test animal, a tissue, a cell culture, or an *in vitro* system.

29. The method according to claim 28, wherein the test system is a test animal.

30. The method according to claim 21, wherein said initiating a ventricular fibrillation inducing sequence is carried out by initiating 4 premature stimuli under conditions effective to initiate an excitatory wave.

31. A method for evaluating the predisposition of a test animal for the induction of ventricular fibrillation from a condition of ventricular tachycardia, said method comprising:

providing a test animal in ventricular tachycardia;

monitoring the electrical stimuli in the heart of the test animal;

determining if each stimulus in groups of 4 stimuli correspond to rest interval values predicted to lead to ventricular fibrillation consistent with the histogram of Figure 3 in "Dynamic Mechanism for Conduction Block in Heart Tissue."

32. A method of identifying treatment candidates as therapeutic strategies for preventing ventricular tachycardia from developing into ventricular fibrillation, said method comprising:

providing a test animal in ventricular tachycardia;

monitoring the electrical stimuli in the heart of the test animal;

determining if an initial 3 stimuli in groups of 4 stimuli in the heart correspond to rest interval values predicted to lead to ventricular fibrillation consistent with the histogram of Figure 3 in "Dynamic Mechanism for Conduction Block in Heart Tissue";

identifying treatment candidates which prevent occurrence of a fourth stimuli corresponding to a rest interval value predicted to lead to ventricular fibrillation consistent with the histogram of Figure 3 in "Dynamic Mechanism for Conduction Block in Heart Tissue";

identifying treatment candidates which prevent said ventricular tachycardia from becoming ventricular fibrillation as therapeutic strategies for prevention of ventricular fibrillation.

33. The method according to claim 32, wherein the treatment candidate is a pharmaceutical compound.

34. The method according to claim 33, wherein the pharmaceutical compound is a calcium channel antagonist.

35. The method according to claim 32, wherein the treatment candidate is one or more electrical impulses.

36. The method according to claim 32, wherein said identifying identifies treatment candidates which achieve velocity restitution values consistent with histograms b and c of Figure 4 in "Dynamic Mechanism for Conduction Block in Heart Tissue" as therapeutic strategies for prevention of ventricular fibrillation.

37. The method according to claim 32, wherein said identifying identifies treatment candidates which achieve potential duration restitution values consistent with histograms b and c of Figure 5 in "Dynamic Mechanism for Conduction Block in Heart Tissue" as therapeutic strategies for prevention of ventricular fibrillation.

38. The method according to claim 32, said identifying identifies treatment candidates which achieve cardiac memory values consistent with histograms b and c of Figure 6 in "Dynamic Mechanism for Conduction Block in Heart Tissue" as therapeutic strategies for prevention of ventricular fibrillation.